

# The risk management approach to macro-prudential policy\*

*Sulkhan Chavleishvili,<sup>(a)</sup> Robert F. Engle,<sup>(b)</sup> Stephan Fahr,<sup>(a)</sup>  
Manfred Kremer,<sup>(a)</sup> Simone Manganelli,<sup>(a)</sup> Bernd Schwaab<sup>(a)</sup>*

<sup>(a)</sup> European Central Bank, Financial Research,

<sup>(b)</sup> New York University Stern School of Business

\*\*\* preliminary conference submission \*\*\*

June 10, 2020

## Abstract

Macro-prudential policy makers need to assess downside risks to the real economy that are caused by severe financial shocks. We propose a structural quantile vector autoregressive model that relates downside risks to the economy to measures of financial stress and medium-term vulnerabilities. In an empirical study of euro area and U.S. data we demonstrate that the dynamic properties of the system differ across quantiles. Counterfactual simulations allow us to construct urgently-needed indicators of macro-prudential policy stance, and to assess when macro-prudential interventions are most likely to be beneficial.

**Keywords:** Growth-at-risk; stress testing; quantile vector autoregression; financial conditions; macro-prudential policy.

**JEL classification:** G21, C33.

---

\*We would like to thank Jacopo Maria D'Andria and Albert Pierres Tejada for excellent research support. E-mail contacts: [sulkhan.chavleishvili@ecb.ecb.europa.eu](mailto:sulkhan.chavleishvili@ecb.ecb.europa.eu); [rengle@stern.nyu.edu](mailto:rengle@stern.nyu.edu); [stephan.fahr@ecb.ecb.europa.eu](mailto:stephan.fahr@ecb.ecb.europa.eu); [manfred.kremer@ecb.ecb.europa.eu](mailto:manfred.kremer@ecb.ecb.europa.eu); [simone.manganelli@ecb.ecb.europa.eu](mailto:simone.manganelli@ecb.ecb.europa.eu); [bernd.schwaab@ecb.ecb.europa.eu](mailto:bernd.schwaab@ecb.ecb.europa.eu). The views expressed in this paper are those of the authors and they do not necessarily reflect the views or policies of the European Central Bank.

# 1 Introduction

A rapidly growing body of research has examined tail risks in macroeconomic outcomes. Most of this work has focused on the risk of significant declines in gross domestic product (GDP), brought about by a deterioration of financial conditions. In particular, growth-at-risk (GaR), the, say, 5% quantile of a predictive GDP distribution, has emerged as a popular measure of downside risk; see e.g. [Adrian et al. \(2020\)](#), [Prasad et al. \(2019\)](#), and [Caldara et al. \(2019\)](#). Both the International Monetary Fund (IMF) as well as the European Central Bank (ECB) now routinely publish GaR estimates for major world economies; see [IMF \(2017\)](#) and [ECB \(2019\)](#). These developments have motivated a proliferation of modeling frameworks to assess the severity of extreme events associated with key economic variables, including single-equation quantile regression (QR) models ([Adrian et al. \(2020\)](#)), panel QR models ([Adrian et al. \(2018\)](#), [Beutel \(2019\)](#), [Brandao-Marques et al. \(2020\)](#)), panel-GARCH models ([Brownlees and Souza \(2019\)](#)), fully non-parametric Kernel regression models ([Adrian et al. \(2020\)](#)), combined linear vector autoregressive (VAR) and single-equation QR models ([Duprey and Ueberfeldt \(2020\)](#)), nonlinear Bayesian VAR models ([Caldara et al. \(2019\)](#), [Carriero et al. \(2020\)](#)), and quantile VAR models ([Chavleishvili and Manganelli \(2019\)](#), [Adrian et al. \(2020\)](#)).<sup>1</sup> Despite GaR's rapid success, however, the question how the statistical notion of downside risk can be made operational for the assessment of risks to financial stability and for macro-prudential policy has received much less attention.

As a result, financial stability policy makers continue to wrestle with urgent open questions. How can financial stability risks be quantified in a meaningful but yet easy-to-communicate way? How large and variable are downside risks to the economy stemming from financial stress and vulnerabilities? Is the macro-economy at all times equally vulnerable to adverse shocks? Is current financial stability policy too loose or too tight? Finally, does actively managing the financial cycle pay off in terms of better macroeconomic outcomes?

This paper addresses the above questions based on an estimated structural quantile vector au-

---

<sup>1</sup>[Manganelli and Kilian \(2008\)](#) show that GaR is a special case of the downside risk measures proposed by [Fishburn \(1977\)](#) in the context of portfolio allocation. They also propose to view a central bank's decision as a risk management problem, requiring the central bank to optimally balance the risks to economic growth and to price stability.

toregressive (QVAR) model. The QVAR model allows us to quantify future risks to economic activity caused by elevated levels of financial stress as well as by economic vulnerability to shocks. We argue that our framework inherits the best features from both the VAR and QR strands of literature: The VAR permits all endogenous variables to interact over time, allows us to be transparent about the identification of structural shocks, and allows us to simulate from the model and compare different counter-factual policy scenarios. By contrast, QR allows the dynamic properties of the system to differ across quantiles, capturing potential asymmetries in the propagation of structural shocks. As a welcome by-product, QR parameter estimates are less sensitive to outliers when compared to their least squares counterparts. This robustness feature can become relevant when financial variables are included in the model and the financial system and the economy face abrupt and large changes. Succinctly put, our QVAR model relates to the single-equation QR approach of [Adrian et al. \(2020\)](#) as the VAR model of [Sims \(1980\)](#) relates to the straightforward single-equation autoregressive approaches of e.g. [Koyck \(1954\)](#) and [Almon \(1965\)](#).

We include measures of financial stress (realized risk) and medium-term vulnerabilities alongside GDP growth in our baseline model. Financial stress is proxied by the ECB's Composite Indicator of Systemic Stress (CISS; see [Hollo et al. \(2012\)](#)), while medium-term vulnerabilities are proxied by [Schüler et al. \(2019\)](#)'s real-time broad financial cycle indicator. Financial stress, the financial cycle, and GDP growth can interact freely in our preferred model specification, and can do so to different extents at different quantiles. The three-variable setup reflects the consideration that financial stability is of concern to policy makers (only) to the extent that it has real economic consequences, e.g. in terms of future employment, consumption, or overall economic activity.

The ECB's definition of financial stability refers to "the risk that the provision of necessary financial products and services by the financial system will be impaired to a point where economic growth and welfare may be materially affected;" see [ECB \(2019\)](#).<sup>2</sup> Downside risk measures thus have the potential to play an important role when assessing and communicating financial stability

---

<sup>2</sup>Similarly, the Financial Stability Board, International Monetary Fund, and the Bank for International Settlements define systemic risk as a "risk of disruption to financial services that is (i) caused by an impairment of all or parts of the financial system, and (ii) has the potential to have serious negative consequences for the real economy;" see [FSB \(2009\)](#).

policy decisions.

Beyond the empirical contribution based on estimated QVAR models this paper also proposes an additional parsimonious downside risk measure to complement GaR. The *average future growth shortfall* (AGS) over a certain prediction horizon  $H$  (say, eight quarters) quantifies the time- $t$  expected average contraction of GDP between  $t + 1$  and  $t + H$  as implied by current financial stress and vulnerabilities. In contrast to GaR, growth shortfall (GS) is a coherent risk measure (see [Artzner et al. \(1999\)](#)) and extends the assessment of risks by taking into account the entire lower tail of the predictive GDP growth distribution. GS can be factored into two intuitive terms: the expected loss conditional on a contraction, and the probability of experiencing a contraction. While both components can be studied separately and can be of interest in their own right, such as in stress test or macroeconomic modeling, AGS summarizes them tractably into one metric and is easily obtained from a QVAR model.

The empirical part of this paper applies our statistical model to both euro area and U.S. data. The paper focuses on euro area data between 1988Q3 and 2018Q4,<sup>3</sup> and analogous tables and figures based on U.S. data between 1973Q1 and 2018Q4 are discussed in a Web Appendix. Our main empirical findings are remarkably similar across the euro area and U.S. samples.

We focus on four empirical findings. First, a variable selection exercise suggests that central bank “intermediate target” variables, such as the financial cycle and (de-trended) money market interest rates, interact closely with GDP growth and financial stress across all quantiles. Other variables, such as the term spread may also play a role, particularly for U.S. data, but are not ranked as highly by model selection criteria. Fortunately, the financial cycle can be influenced to at least some extent by macro-prudential (and monetary) policy instruments. Our downside risk estimates are not particularly sensitive to the exclusion of short-term interest rates; we therefore use the more parsimonious trivariate model specification for most of our results.

Second, the dynamic properties of the system differ significantly across quantiles. A formal Wald test rejects the pooling, or parameter homogeneity, restrictions implied by a linear VAR

---

<sup>3</sup>Counterfactual data preceding the formation of the euro area (pre-1999) is obtained from an internal ECB database.

specification for our data at any reasonable confidence level. The QVAR is instead characterized by substantial asymmetries. For example, a shock to financial stress (CISS) shifts the left tail of future GDP towards more negative values, while leaving its conditional median and right tail approximately unaffected. As a second example, growing financial vulnerabilities (the financial cycle) shift the right tail of future financial stress towards higher values, while shifting its left tail further to the left. As in [Adrian et al. \(2020\)](#), macro-financial interactions imply that the upper quantiles of predictive GDP growth distribution are less volatile than its lower quantiles.

Our model-implied downside risk measures are strongly sensitive to the inclusion of financial variables. Not only do downside risks associated with the global financial crisis between 2008 and 2009 decline much later, and to a lesser extent, when financial stress is missing, but in addition the downside risks associated with the 2010 – 2012 euro area sovereign debt crisis are missed almost entirely when financial stress (CISS) is not included in the model.

Third, we find that the euro area economy is not equally resilient to the same sequence of adverse financial shocks at all times. The asymmetries (nonlinearities) uncovered in the data suggest that our QVAR model provides a natural environment to perform repeated model-based macro-prudential stress tests for the economy as a whole. We here understand stress testing as a forecast of what would happen to all variables in the system should it be subjected to a fixed sequence of adverse shocks. We find that downside risks conditional on future adverse real and financial shocks shoot up during crises, and are driven during the crisis by spikes in our financial stress indicator and by reductions in the vulnerability indicator. Our measure of downside risk can be used as a quantitative yardstick to calibrate the size of macro-prudential capital and liquidity buffers.

The Stoic Roman philosopher Seneca once observed that “When pleasures have corrupted both mind and body, nothing seems tolerable – not because the suffering is hard, but because the sufferer is soft.”<sup>4</sup> When applied to financial sector stress testing, the quote could read: “When excess leverage and bad credit growth have sufficiently weakened financial stability, then no shock to financial conditions seems tolerable – not because the shock is large, but because the system

---

<sup>4</sup>Seneca, De Ira, Liber II, XXV, 3.

has become financially vulnerable.” In QVAR-based stress tests, the impact of a shock to financial conditions (stress) depends not only on its initial severity, but also on the endogenous, asymmetric responses of all other variables in the system. Allowing for such feedback and asymmetries is crucial when subjecting the system to a sequence of joint tail shocks. To counteract the feedback and the asymmetries we argue that macro-prudential policy should act in a counter-cyclical fashion by releasing requirements such as capital and liquidity buffers when downside risk is exceptionally high and tightening when downside risk is exceptionally low.

Finally, we find that managing the financial cycle is not obviously costly in terms of expected future economic growth. In a thought experiment, we ask the question: what would euro area real GDP growth have been had a macro-prudential policy maker been able to perfectly mitigate the contributions from the financial cycle, while leaving the structural shocks to the other variables unchanged.<sup>5</sup> We find that in the counterfactual exercise both mean and median of GDP growth are higher, growth volatility is lower as negative and positive extreme realizations disappear, and growth is less skewed towards the downside. Welfare calculations from stabilizing the financial cycle can be based on the macro-prudential objective function suggested by [Carney \(2020\)](#). The associated welfare gains can be positive or negative, and are most positive in exuberant times when the financial cycle is above its conditional median.

Our findings can have important implications for the design of central banks’ financial stability policies. As a first key takeaway, macro-prudential policies, rather than monetary policy, should be first in line to address future financial stability risks. In our thought experiment, adjusting macroprudential policies counter-cyclically to manage the financial cycle is associated with non-negligible welfare gains. This is in line with e.g. [Svensson \(2017\)](#), who advises against leaning against excessive credit growth using short-term interest rates and favours macro-prudential instruments instead. Second, model-based stress tests can give additional, quantitative information when to build up macro-prudential capital buffers and when to release them. Such macro model-based stress test outcomes can complement early warning indicators such as the credit-to-GDP-ratio gap

---

<sup>5</sup>For a detailed discussion of the assumptions underlying this thought experiment we refer to the main text.

that has traditionally informed the calibration of the counter-cyclical buffer. Doing so may help overcome a potential “inactivity-bias,” according to which few jurisdictions have set their counter-cyclical capital buffers to above-zero levels from the buffer’s inception in 2014 to late 2019.<sup>6</sup>

We proceed as follows. Section 2 defined our downside risk measures and presents the statistical model. Section 3 introduces our data. Section 4 applies the model to euro area and U.S. data. Section 5 concludes. A Web Appendix provides further technical and empirical results.

## 2 Statistical model

### 2.1 Measures of downside risk

The ECB’s definition of financial stability refers to “*the risk that the provision of necessary financial products and services by the financial system will be impaired to a point where economic growth and welfare may be materially affected.*” Our point of departure is that financial stability is of concern to policy makers (only) to the extent that it has real economic consequences, e.g. in terms of future employment, consumption, or overall economic activity.

We define three measures of adverse real economic impact arising from financial stress and systemic vulnerabilities. Each measure is of interest in different settings. Our first measure of adverse impact is *growth-at-risk* ( $\text{GaR}_{t,t+h}^\gamma$ ) at confidence level  $\gamma \in (0, 1)$ , defined implicitly as

$$\mathbb{P} [y_{t+h} \leq \text{GaR}_{t,t+h}^\gamma | \mathcal{F}_{1t}] = \gamma, \quad (1)$$

where  $y_t$  denotes the quarterly annualized real GDP growth rate between time  $t - 1$  and  $t$ , and  $h = 1, \dots, H$  denotes a certain prediction horizon. The information set  $\mathcal{F}_{1t}$  contains all data known at time  $t$ ; see Section 2.2 below. In words,  $\text{GaR}_{t,t+h}^\gamma$  is defined such that the probability of quarterly annualized output growth at  $t + h$  falling below  $\text{GaR}_{t,t+h}^\gamma$  is  $\gamma$ .

---

<sup>6</sup>At the end of 2018, 19 out of 28 European Union countries, and 15 out of 19 euro area countries, had counter-cyclical capital buffers set at zero; see Web Appendix A for details.

Our second measure of adverse real economic impact is *growth shortfall* (GS), defined as

$$\begin{aligned}\text{GS}_{t,t+h}^\tau &= \int_{-\infty}^{\tau} y_{t+h} dF_{t,t+h}(y_{t+h}) \\ &= \mathbb{E}[y_{t+h} | y_{t+h} < \tau, \mathcal{F}_{1t}] \times \mathbb{P}[y_{t+h} < \tau | \mathcal{F}_{1t}],\end{aligned}\quad (2)$$

where  $F_{t,t+h}$  is a time- $t$  conditional cumulative distribution function (cdf),  $\mathbb{E}[\cdot | \mathcal{F}_{1t}]$  denotes a time- $t$  conditional expectation, and the threshold  $\tau \in \mathbb{R}$  could be set to a low conditional quantile, say  $\tau = \text{GaR}_{t,t+h}^\gamma$ . If so, then the first factor in (2) coincides with the familiar notion of expected shortfall; see e.g. [McNeil et al. \(2005, Ch. 2\)](#). Alternatively, it could be set to a certain unconditional quantile, or be set to zero. If  $\tau = 0$ , then GS (2) corresponds to the economic question: what is the time  $t$ -expected contraction of the economy at time  $t + h$ . GS factors into two terms: the expected growth rate given a contraction, and the conditional probability of witnessing a contraction.<sup>7</sup>

Our final measure of adverse real economic impact is the *average future growth shortfall* (AGS) between  $t + 1$  and  $t + H$ , defined as

$$\overline{\text{GS}}_{t,t+1:t+H}^\tau = H^{-1} \sum_{h=1}^H \text{GS}_{t,t+h}^\tau. \quad (3)$$

If  $\tau = 0$ , then the AGS corresponds to the question: what is the average future expected contraction of the economy between  $t + 1$  and  $t + H$ .

All above risk measures are economically intuitive and straightforward to communicate. Risk measures (2) and (3), however, have theoretical and practical advantages over (1). First, expected shortfall-based measures are coherent risk measures, while any single quantile in isolation is not ([Artzner et al. \(1999\)](#)). For example, GS contributions are sub-additive, while GaR contributions are not. This feature is desirable if one, for instance, wants to study sector contributions to aggregate GDP at risk. Second, while all above risk measures (1) – (3) can take into account the asymmetric impact of financial variables on the economy, only (2) and (3) take into account the

---

<sup>7</sup>To see this, note that  $\mathbb{E}[y_{t+h} | y_{t+h} < \tau, \mathcal{F}_{1t}] \equiv \frac{\int_{-\infty}^{\tau} y_{t+h} \cdot 1_{\{y_{t+h} < \tau\}} dF_{t,t+h}(y_{t+h})}{\int_{-\infty}^{\tau} 1_{\{y_{t+h} < \tau\}} dF_{t,t+h}(y_{t+h})} = \frac{\int_{-\infty}^{\tau} y_{t+h} dF_{t,t+h}(y_{t+h})}{\mathbb{P}[y_{t+h} < \tau | \mathcal{F}_{1t}]}$ .

entire left tail.

When considering financial stability policies aimed at containing downside risks, then the expected growth rate of the economy, as well as the upper quantiles of future GDP growth, should not be unduly affected. For later reference, we define the *growth longrise*<sup>8</sup> (GL) as the complement to GS,

$$\begin{aligned}\text{GL}_{t,t+h}^\tau &= \int_\tau^\infty y_{t+h} dF_{t,t+h}(y_{t+h}) \\ &= \mathbb{E}[y_{t+h} | y_{t+h} > \tau, \mathcal{F}_{1t}] \times \mathbb{P}[y_{t+h} > \tau | \mathcal{F}_{1t}].\end{aligned}\quad (4)$$

If  $\tau = 0$ , then (4) corresponds to the question: what is the time- $t$  expected expansion of the economy between  $t + h - 1$  and  $t + h$ . Similarly to GS, the growth longrise (4) captures the expected growth given an expansion, and the conditional probability of experiencing an expansion. Given the complementarity between GS and GL, their sum equals the expected growth rate of the economy between  $t + h - 1$  and  $t + h$ ,

$$\begin{aligned}\mathbb{E}[y_{t+h} | \mathcal{F}_{1t}] &= \int_{-\infty}^\infty y_{t+h} dF_{t,t+h}(y_{t+h}) \\ &= \int_{-\infty}^\tau y_{t+h} dF_{t,t+h}(y_{t+h}) + \int_\tau^\infty y_{t+h} dF_{t,t+h}(y_{t+h}) \\ &= \text{GS}_{t,t+h}^\tau + \text{GL}_{t,t+h}^\tau.\end{aligned}$$

Analogously to (3), we also define the *average future growth longrise* (AGL) between  $t + 1$  and  $t + H$  as

$$\overline{\text{GL}}_{t,t+1:t+H}^\tau = H^{-1} \sum_{h=1}^H \text{GL}_{t,t+h}^\tau. \quad (5)$$

Finally, let  $\bar{y}_{t,t+1:t+H} = H^{-1} \sum_{h=1}^H y_{t,t+h}$  be the average future economic growth rate between  $t + 1$  and  $t + H$ . Since (2) and (4) are linear, the expected future growth rate of the economy between  $t + 1$  and  $t + H$  is  $\mathbb{E}[\bar{y}_{t,t+1:t+H} | \mathcal{F}_{1t}] = \overline{\text{GS}}_{t,t+1:t+H}^\tau + \overline{\text{GL}}_{t,t+1:t+H}^\tau$ . As a result, expected

---

<sup>8</sup>The term longrise was coined by [Adrian et al. \(2020\)](#) as the antonym to shortfall.

average future growth can be read off any figure reporting  $\overline{\text{GS}}_{t,t+1:t+H}^\tau$  and  $\overline{\text{GL}}_{t,t+1:t+H}^\tau$  by adding the two lines.

Different econometric techniques can be used to estimate (1) – (5). We will estimate it from a structural quantile vector autoregressive (QVAR) model; see Section 2.2. One advantage of quantile regression is that it allows financial variables to have a different impact on different parts of the distribution. This is relevant, as financial stress may impact the left tail of output growth much more than, say, its upper quantiles.<sup>9</sup> QVAR models allow all variables to interact at times  $t + 1, t + 2, \dots, t + H$ , and to do so to different extents at different quantiles.

## 2.2 Quantile vector autoregression

This section provides a concise exposition of the structural quantile vector autoregressive (QVAR) model of [Chavleishvili and Manganelli \(2019\)](#).

We observe a series of random variables  $\{\tilde{x}_t : t = 1, \dots, T\}$ , where  $\tilde{x}_t \in \mathbb{R}^n$  is an  $n$ -vector with  $i^{\text{th}}$  element denoted by  $\tilde{x}_{it}$  for  $i \in \{1, \dots, n\}$  and  $n \in \mathbb{N}$ . While the baseline empirical model in Section 4 considers three variables, we here develop intuition based on a simpler bivariate model for the data vector  $\tilde{x}_t = (y_t, s_t)'$ , where  $y_t$  is the quarterly annualized real GDP growth between  $t - 1$  and  $t$ , and  $s_t$  is a coincident indicator of systemic financial stress. For any arbitrary but fixed quantile  $\gamma$ , the QVAR model of order 1 is given by

$$\tilde{x}_{t+1} = \omega^\gamma + A_0^\gamma \tilde{x}_{t+1} + A_1^\gamma \tilde{x}_t + \epsilon_{t+1}^\gamma \quad (6)$$

$$\mathbb{P}(\epsilon_{i,t+1}^\gamma < 0 | \mathcal{F}_{it}) = \gamma, \quad \text{for } i = 1, \dots, n, \quad (7)$$

where the vector of structural quantile residuals is given by  $\epsilon_t^\gamma \equiv [\epsilon_{1t}^\gamma, \dots, \epsilon_{nt}^\gamma]'$ . Recursive identification is achieved by restricting the  $[n \times n]$  matrix  $A_0^\gamma$  to be lower triangular with zeros along the main diagonal. The presence of contemporaneous dependent variables on the right-hand side of

---

<sup>9</sup>Asymmetric responses of the real economy to large adverse financial shocks are in line with the empirical findings in [Adrian et al. \(2020\)](#), but also with recent theoretical advances. Asymmetric responses can e.g. be explained by occasionally binding financing constraints; see e.g. [Bianchi \(2011\)](#) and [He and Krishnamurthy \(2019\)](#).

(6) requires us to be precise about the available information at any time and for each variable. We work with an incremental information set that increases one scalar observation at a time,

$$\mathcal{F}_{1t} = \{\tilde{x}_t, \tilde{x}_{t-1}, \dots\} \quad (8)$$

$$\mathcal{F}_{it} = \{\tilde{x}_{1,t+1}, \dots, \tilde{x}_{i-1,t+1}, \tilde{x}_t, \tilde{x}_{t-1}, \dots\} \text{ for } i \in \{2, \dots, n\}. \quad (9)$$

In words,  $\mathcal{F}_{1t}$  contains only variables observed up to time  $t$ . The information sets  $\mathcal{F}_{it}$  for  $i > 1$  contain increasingly more information about variables observed at  $t + 1$ .<sup>10</sup>

We may wish to consider multiple quantiles of multiple variables at the same time. To do this in a compact way, we consider  $p$  distinct quantiles  $0 < \gamma_1 < \dots < \gamma_p < 1$ , for  $p \in \mathbb{N}$ , not necessarily equidistant. In addition, we let  $x_t \equiv [\iota_p \otimes \tilde{x}_t]$  denote the vector stacking  $p$  times the dependent variables  $\tilde{x}_t$ , where  $\iota_p$  is a  $p$ -vector of ones. The stacked QVAR model of order 1 is then given by

$$x_{t+1} = \omega + A_0 x_{t+1} + A_1 x_t + \epsilon_{t+1} \quad (10)$$

$$\mathbb{P}(\epsilon_{i,t+1}^{\gamma_j} < 0 | \mathcal{F}_{it}) = \gamma_j, \quad \text{for } i = 1, \dots, n, \quad j = 1, \dots, p \quad (11)$$

where the vector of structural quantile residuals is given by  $\epsilon_t \equiv [\epsilon_{1t}^{\gamma_1}, \dots, \epsilon_{nt}^{\gamma_1}, \dots, \epsilon_{1t}^{\gamma_p}, \dots, \epsilon_{nt}^{\gamma_p}]'$ . The  $[np \times np]$  matrices  $A_0$  and  $A_1$  are block diagonal to avoid trivial multicollinearity problems. The model (10) – (11) is essentially a convenient way to stack  $p$  quantile-specific QVAR models (6) – (7).

An explicit example may be instructive. Let's recall the above bivariate example  $\tilde{x}_t = (y_t, s_t)'$  of real GDP growth and financial stress, and consider  $p = 2$  quantiles for simplicity, 0.10 and 0.90. The system (10) – (11) can then be written as

---

<sup>10</sup>For a similar incremental conditioning approach in a different setting see e.g. [Koopman and Durbin \(2000\)](#).

$$\begin{aligned}
\begin{bmatrix} y_{t+1} \\ s_{t+1} \\ y_{t+1} \\ s_{t+1} \end{bmatrix} &= \begin{bmatrix} \omega_y^1 \\ \omega_s^1 \\ \omega_y^9 \\ \omega_s^9 \end{bmatrix} + \begin{bmatrix} 0 & 0 & 0 & 0 \\ a_{021}^1 & 0 & 0 & 0 \\ 0 & 0 & 0 & 0 \\ 0 & 0 & a_{021}^9 & 0 \end{bmatrix} \begin{bmatrix} y_{t+1} \\ s_{t+1} \\ y_{t+1} \\ s_{t+1} \end{bmatrix} \\
&+ \begin{bmatrix} a_{11}^1 & a_{12}^1 & 0 & 0 \\ a_{21}^1 & a_{22}^1 & 0 & 0 \\ 0 & 0 & a_{11}^9 & a_{12}^9 \\ 0 & 0 & a_{21}^9 & a_{22}^9 \end{bmatrix} \begin{bmatrix} y_t \\ s_t \\ y_t \\ s_t \end{bmatrix} + \begin{bmatrix} \epsilon_{y,t+1}^1 \\ \epsilon_{s,t+1}^1 \\ \epsilon_{y,t+1}^9 \\ \epsilon_{s,t+1}^9 \end{bmatrix} \quad (12)
\end{aligned}$$

Here, the ordering of the observations in (12) reflects the assumption that the financial stress variable  $s_t$  can react contemporaneously to macroeconomic shocks, while real output growth  $y_t$  can react to financial shocks only with a lag. Such assumptions are standard in the empirical literature; see e.g. [Gilchrist and Zakrajsek \(2012\)](#).

### 2.3 Forecasting

This section explains how forecasts can be generated from the stacked QVAR model (10) – (11) without invoking parametric assumptions on  $\epsilon_{t+1}$ .

It is helpful to introduce the conditional quantile operator  $Q_{it}^{\gamma_j}(x_{k,t+1})$ , where  $x_{k,t+1}$  is the  $k$ -th element of  $x_{t+1}$ ,  $k = 1, \dots, np$ . Given information set  $\mathcal{F}_{it}$ , the operator is implicitly defined by

$$\mathbb{P}(x_{k,t+1} < Q_{it}^{\gamma_j}(x_{k,t+1}) | \mathcal{F}_{it}) = \gamma_j, \quad \text{for } j = 1, \dots, p.$$

In words,  $Q_{it}^{\gamma_j}(x_{k,t+1})$  returns the  $\gamma_j$  quantile of random variable  $x_{k,t+1}$  conditional on  $\mathcal{F}_{it}$ . The element  $x_{k,t+1}$  is random because it depends on its own shock at time  $t + 1$ , but also, potentially, on shocks to earlier elements  $x_{1,t+1}, \dots, x_{k-1,t+1}$ .

To build intuition first, let us return to the simple bivariate example (12) with  $n = p = 2$ . Let's

assume we are interested in forecasting, say, the 0.9 quantile of the financial stress variable  $s_{t+1}$ .

The fourth equation of (12), corresponding to the 0.9 quantile of  $s_{t+1}$ , is

$$\begin{aligned}
s_{t+1} &= \omega_s^{\cdot 9} + a_{021}^{\cdot 9}[\omega_y^{\cdot 9} + a_{11}^{\cdot 9}y_t + a_{12}^{\cdot 9}s_t + \epsilon_{y,t+1}^{\cdot 9}] + a_{21}^{\cdot 9}y_t + a_{22}^{\cdot 9}s_t + \epsilon_{s,t+1}^{\cdot 9} \\
&= \omega_s^{\cdot 9} + a_{021}^{\cdot 9}\omega_y^{\cdot 9} + (a_{021}^{\cdot 9}a_{11}^{\cdot 9} + a_{21}^{\cdot 9})y_t + (a_{021}^{\cdot 9}a_{12}^{\cdot 9} + a_{22}^{\cdot 9})s_t + a_{021}^{\cdot 9}\epsilon_{y,t+1}^{\cdot 9} + \epsilon_{s,t+1}^{\cdot 9} \\
&= q_{st}^{\cdot 9} + a_{021}^{\cdot 9}\epsilon_{y,t+1}^{\cdot 9} + \epsilon_{s,t+1}^{\cdot 9}
\end{aligned} \tag{13}$$

where  $q_{st}^{\cdot 9} \equiv \omega_s^{\cdot 9} + a_{021}^{\cdot 9}\omega_y^{\cdot 9} + (a_{021}^{\cdot 9}a_{11}^{\cdot 9} + a_{21}^{\cdot 9})y_t + (a_{021}^{\cdot 9}a_{12}^{\cdot 9} + a_{22}^{\cdot 9})s_t$  depends only on deterministic parameters to be estimated and variables observed at time  $t$ . We note that  $Q_{st}^{\cdot 9}(\epsilon_{s,t+1}^{\cdot 9}) = 0$  because of the identifying restriction (11), stating  $\mathbb{P}(\epsilon_{s,t+1}^{\cdot 9} < 0 | \mathcal{F}_{st}) = 0.9$  when  $\mathcal{F}_{st} = \{y_{t+1}, y_t, s_t, \dots\}$ . In addition,  $q_{st}^{\cdot 9} + a_{021}^{\cdot 9}\epsilon_{y,t+1}^{\cdot 9} | \mathcal{F}_{st}$  is non-random. As a result,  $Q_{st}^{\cdot 9}(s_{t+1}) = q_{st}^{\cdot 9} + a_{021}^{\cdot 9}\epsilon_{y,t+1}^{\cdot 9}$ . This quantity is, however, not too helpful because it's still a random variable at time  $t$ . We therefore keep on taking quantiles. Using the identifying restriction (11) again,  $Q_{yt}^{\cdot 9}(\epsilon_{y,t+1}^{\cdot 9}) = 0$ , yields  $Q_{yt}^{\cdot 9}(Q_{st}^{\cdot 9}(s_{t+1})) = q_{st}^{\cdot 9}$ . As a result,  $q_{st}^{\cdot 9}$  is our sought-after forecast of the 0.9 quantile of  $s_{t+1}$ , and is easily computed. This approach of iterated quantiles can be repeated for any potentially remaining variables in  $x_{t+1}$ . Following that, the approach can be repeated for future variables in  $x_{t+h}$  for  $h > 1$ .<sup>11</sup>

The above reasoning can be formalized. The scalar operators  $Q_{it}^{\cdot j}(x_{k,t+1})$  can be combined into a vector version, with quantile operators nesting each other up to  $n$  times. The vector operators can again be sequentially combined, up to  $H$  times. In the end, the  $[np \times 1]$ -vector of quantile forecasts at time  $t$  associated with process (10), for  $h = 1, \dots, H$ , can be obtained quite straightforwardly as

$$\hat{x}_{t+h} = \sum_{j=0}^{h-1} B^j \nu + B^h x_t, \tag{14}$$

where  $\nu = (I_{np} - A_0)^{-1} \omega$  and  $B = (I_{np} - A_0)^{-1} A_1$ . We refer to [Chavleishvili and Manganeli \(2019\)](#) for the proof. It is easily verified that  $\hat{x}_{4,t+1}$  (i.e., the fourth element of  $\hat{x}_{t+1}$ , obtained using

<sup>11</sup> This example implicitly assumes that  $a_{021}^{\cdot 9}$  is positive. If not, then the 0.9 conditional quantile and the 0.1 conditional quantile cross. This is because, when  $a_{021}^{\cdot 9} < 0$ , then  $\mathbb{P}(a_{021}^{\cdot 9}\epsilon_{y,t+1}^{\cdot 9} < 0) = \mathbb{P}(\epsilon_{y,t+1}^{\cdot 9} > 0) = 1 - \mathbb{P}(\epsilon_{y,t+1}^{\cdot 9} < 0) = 1 - 0.9 = 0.1$ . If this happens we reorder (relabel) the quantiles accordingly.

(14)) coincides with  $q_{st}^9$  as defined below (13).

A drawback of (14), for  $H \geq 2$ , is that it continues to use the same quantile-specific parameters. In other words, it keeps sending  $\hat{x}_{t+h}$  down the same path. It therefore cannot be used directly to explore the entire growing tree of potential outcomes  $\hat{x}_{t+h}$  for all  $h = 1, \dots, H$ . The next section discusses a simulation approach that does not suffer from this drawback.

## 2.4 Semi-parametric risk measurement

This section explains how we obtain the time- $t$  downside risk measures introduced in Section 2.1 from our semi-parametric structural QVAR model (10) – (11) using simulation methods. To this end we rely on a growing literature on simulation methods for quantile regression; see e.g. Hahn (1995) and Koenker (2005, Ch. 2.6).

When we defined the structural QVAR model for an arbitrary quantile  $\gamma$  as (6) – (7), and insisted that the model holds for all  $\gamma \in (0, 1)$ , we effectively specified a complete stochastic mechanism for generating the one-step ahead variable  $\tilde{x}_{t+1}$  conditional on time- $t$  information and deterministic parameters. Recall that any scalar response variable  $\tilde{x}_{i,t+1}$ ,  $i = 1, \dots, n$ , with conditional cdf  $F_{i,t,t+1}$ , can be simulated by generating a standard uniform variable  $u_{i,t+1} \sim U[0, 1]$ , and then setting  $\tilde{x}_{i,t+1} = F_{i,t,t+1}^{-1}(u_{i,t+1})$ . Thus, in model (6) – (7),  $\tilde{x}_{i,t+1}$  can be simulated setting  $\tilde{x}_{i,t+1} = \omega_i^{u_{i,t+1}} + A_{0,i}^{u_{i,t+1}} \tilde{x}_{i,t+1} + A_{1,i}^{u_{i,t+1}} \tilde{x}_{i,t}$ , where  $\omega_i^{(\cdot)}$ ,  $A_{0,i}^{(\cdot)}$ , and  $A_{1,i}^{(\cdot)}$  denote the  $i$ -th row of  $\omega^\gamma$ ,  $A_0^\gamma$ , and  $A_1^\gamma$ , respectively, evaluated at  $\gamma = u_{i,t+1}$ . This procedure allows us to generate the  $\tilde{x}_{t+h}$ , recursively, for  $h = 1, \dots, H$ , conditional on the relevant information sets.

We sketch our simulation algorithm here, and refer to Web Appendix B.4 for details. Let  $t = 1, \dots, T$  denote any time in our sample. We obtain time- $t$  conditional downside risk measures by simulating forward  $S = 10,000$  potential future paths for all  $n$  variables in  $\tilde{x}_{i,t+h}$ ,  $h = 1, \dots, 8$  quarters ahead. The simulations are based on inverse cdf-sampling as described above, and use the one-step-ahead recursion (6). At each  $t + h$ , we calculate  $GS_{t,t+h}^\tau$  and  $GL_{t,t+h}^\tau$  by evaluating the sample analogues of (2) and (4). At the end of each simulation, we average across  $S$  to obtain downside risk measures  $\bar{GS}_{t,t+1:t+h}^\tau$  and  $\bar{GL}_{t,t+1:t+h}^\tau$ ; see (3) and (5). Finally, all estimates are

averaged over the  $S$  simulation draws.

Rather than re-estimating the model parameters within each simulation and for each variable using  $\gamma_i = u_{i,t+h}$ , it is computationally advantageous to discretize the support of the standard uniform random variable with an appropriately chosen grid  $0 < \gamma_1 < \dots < \gamma_p < 1$ , and to estimate all parameters once and for all in the beginning based on the full sample. We then use the parameter estimates associated with the closest selected quantile in any simulation. We use  $p = 20$  grid-points for this purpose,  $0 < 0.025, 0.075, \dots, 0.925, 0.975 < 1$ , each at the midpoint of  $1/20$ th of the unit interval. These grid-points are symmetric about the median, and yield equiprobable simulation paths. Crossing quantiles (see footnote 11) are not an issue since we move through the tree at random. Our downside risk estimates reported in Section 4.4 are robust to increasing the number of grid-points, and to interpolating parameter estimates between quantiles.

## 2.5 Counterfactual scenarios

This section explains how counterfactual scenarios can be obtained from the QVAR model (10) – (11). We use counterfactual scenarios repeatedly below, e.g. when considering a market-based stress test against 2008Q1–2009Q2-sized financial shocks in Section 4.5, and when studying the benefits vs. cost from tightening macro-prudential policy stance in Sections 4.6.

Rather than moving through the complete tree of potential future values of  $\tilde{x}_{t+h}$  at random, as explained in Section 2.4, we may at other times wish to consider only one path in isolation. One path in isolation can also be thought of as a ‘counterfactual scenario,’ or model-based thought experiment that conditions on an arbitrary but fixed sequence of future shocks.

The quantile of each element of the vector  $x_{t+1}$  at time  $t$  is a random variable, as, except for the first element, it depends on the contemporaneous shocks of the other variables. Given the recursive identification assumption, we can forecast the quantiles conditional on any desired quantile shock realization. To this end we define a sequence of selection matrices  $\{S_{t+h}^{\gamma^h}\}_{h=1}^H$ , with typical  $[n \times np]$  element  $S_{t+h}^{\gamma^h}$  selecting specific quantile shocks from the  $[np \times 1]$  vector  $\epsilon_{t+h}$  (see (10)), one shock

for each variable  $i$ :

$$S_{t+h}^{\gamma^i} \epsilon_{t+h} \equiv [\epsilon_{1,t+h}^{\gamma^i}, \dots, \epsilon_{n,t+h}^{\gamma^i}]', \quad (15)$$

for  $\gamma_{t+h}^i \in \{\gamma_1, \dots, \gamma_p\}$  and  $i \in \{1, \dots, n\}$ , selecting the variable-specific shocks to be set to zero.<sup>12</sup> By (6)–(7), the quantile forecast of  $\tilde{x}_{t+1}$ , conditional on setting the quantile shocks identified by the matrix  $S_{t+h}^{\gamma^i}$  to zero, is

$$\hat{\tilde{x}}_{t+h} | S_{t+h}^{\gamma^i} = C_{t+h}(\omega + A_1 x_{t+h-1}) \quad (16)$$

where  $C_{t+h} \equiv (I_n - S_{t+h}^{\gamma^i} A_0 \bar{S})^{-1} S_{t+h}^{\gamma^i}$ , and where  $\bar{S}$  is a  $[np \times n]$  matrix such that  $x_{t+h} = \bar{S} S_{t+h}^{\gamma^i} x_{t+h}$ .<sup>13</sup>

Given the above sequence  $\{S_{t+h}^{\gamma^i}\}_{h=1}^H$ , it is now possible to iterate the system (16) forward to obtain forecasts of the dependent variables  $\tilde{x}_{t+h}$  at any future point  $h$  conditional on the specified counterfactual scenario.

## 2.6 Comparing multiple counterfactual scenarios

An objective function is useful to compare the outcomes implied by two or more counterfactual scenarios.

Suppose the macro-prudential authority has an instrument (or vector of instruments)  $c_t$  that can be used to influence the predictive growth distribution. This influence can be direct ( $c_t \rightarrow y_{t+1}$ ) or indirect (e.g.,  $c_t \rightarrow s_t \rightarrow y_{t+1}$ ). The QVAR structure allows us to capture both types of transmission. A convenient way to penalize downside risk is given by

$$\max_{\{c_{t+h}\}_{h=1}^{\infty}} \sum_{h=1}^{\infty} \beta^h (GL_{t,t+h}(c_{t+h}) + \lambda GS_{t,t+h}(c_{t+h})) \quad (17)$$

where  $\lambda > 1$  is a weight determining the aversion to negative realisations of output growth,  $\beta$  is an

<sup>12</sup>Recall that zero is not a neutral value except for the median; see (11).

<sup>13</sup> $\bar{S}$  consists of stacked identity matrices and is always available and unique. The selection of variable-specific quantiles via (15) does not lead to a loss of information.

intertemporal discount factor, and  $GS_{t,t+h}$  is a negative number.

The objective function (17) is reminiscent of the mean with downside risk model in asset allocation; see e.g. Fishburn (1977). Since  $\mathbb{E}[y_{t+h}|\mathcal{F}_{1t}] = GS_{t,t+h}^\tau + GL_{t,t+h}^\tau$ , see Section 2.1, (17) can be rewritten in terms of expected future economic growth instead of upper quantiles to future growth. If so, the objective function (17) is equal to the expression suggested by Carney (2020),

$$\max_{\{c_{t+h}\}_{h=1}^{\infty}} \sum_{h=1}^{\infty} \beta^h (\mathbb{E}_t(y_{t+h}(c_{t+h})) + (\lambda - 1)GS_{t,t+h}(c_{t+h})), \quad (18)$$

trading off future trend growth against downside risks to the economy. We use (18) to compare the benefits from adopting an active financial stability policy with the benefits from adopting a passive financial stability policy in Section 4.6 below.

## 3 Data

### 3.1 Macroeconomic data pre-1999

Structural QVAR models require a sufficiently large sample size to ensure that its parameters can be estimated with adequate precision. At least two challenges are present, however, when working with euro area macro data in practice. First, the euro area celebrated its 20th anniversary merely in 2019. When working with quarterly data,  $T = 4 \times 20 = 80$  is at the lower end of what is required for a meaningful empirical study of macro-financial interactions at different quantiles. Second, euro area membership has been expanding over time, from initially 11 countries in 1999 to 19 countries in 2015. Changes in euro area aggregate data stemming from new countries joining, rather than, say, from changes in financial conditions or growing vulnerabilities, would severely complicate any empirical analysis.

Fortunately, both problems can be addressed. During the ECB's early years, pre-1999 macro-financial time series data were urgently needed for monetary policy analysis. Against this background counterfactual data were constructed "as if" the euro area had already consisted earlier; see

e.g. [Fagan et al. \(2001\)](#)). Such pre-1999 euro area data is publicly available.<sup>14</sup> We obtain real GDP growth data from 1988Q3 to 2018Q4 from this source, resulting in  $T = 121$ .

### 3.2 Composite indicator of systemic stress

This section introduces the ECB's composite indicator of systemic stress (CISS). The CISS is computed for the euro area as a whole. It includes 15 raw, mainly market-based financial stress measures that are split equally into five categories: financial intermediaries, money markets, equity markets, bond markets, and foreign exchange markets; see [Web Appendix C.1](#) and [Hollo et al. \(2012\)](#) for details. Each category is summarized by a sub-index. The sub-indices are subsequently aggregated to a single time series in a way that takes their time-varying cross-correlations into account. As a result, the CISS takes higher values when stress prevails in several market segments *at the same time*, capturing the idea that financial stress is more systemic, and more dangerous for the economy as a whole, whenever financial instability spreads widely across different segments of the financial system. [Web Appendix C.1](#) provides a listing of all included data series. The CISS is updated regularly and publicly available.<sup>15</sup>

The left panel of [Figure 1](#) reports euro area GDP growth along with the CISS between 1988Q3 and 2018Q4. High values of the CISS are observed during the recession in 1992, the global financial crisis between 2008 and 2009, and during the euro area sovereign debt crisis between 2010 and 2012. In each case, elevated financial stress is associated with negative GDP growth.

### 3.3 Real-time estimates of the financial cycle

For future reference, this section briefly discusses [Schüler et al. \(2019\)](#)'s real-time financial cycle indicator. The construction of the indicator mirrors that of the CISS; see [Web Appendix \(C.2\)](#) for details and [Figure 1](#) for an illustration. Their indicator takes high values when *i*) total non-financial

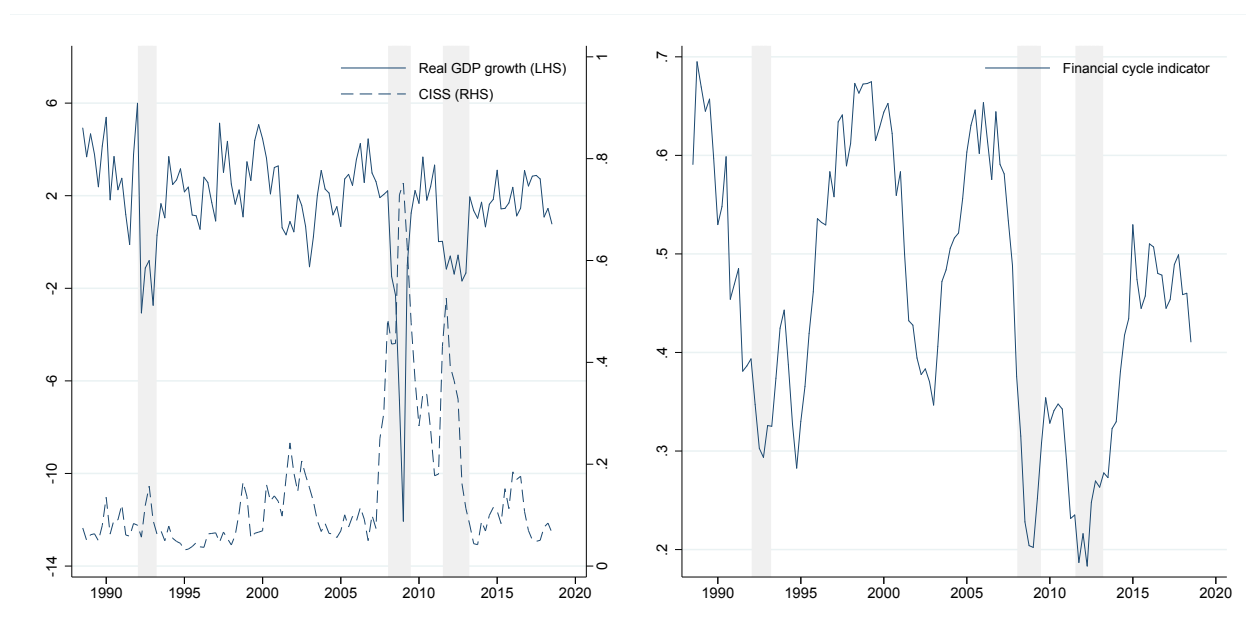
---

<sup>14</sup><https://eabcn.org/page/area-wide-model>. In its most recent version, the database adopts a fixed euro area composition approach, constructing aggregate data series as if the euro area had always consisted of its current (end-of-sample) 19 members. Most variables are available from 1970Q1 onwards. The further back, however, the more uncertain the data quality.

<sup>15</sup><https://sdw.ecb.europa.eu/>

**Figure 1: Euro area real GDP growth rate, CISS, and financial cycle indicator**

Left panel: The GDP growth rate is annualized (left scale). The CISS varies between 0 and 1 by construction (right scale). Right panel: The real-time broad financial cycle indicator of [Schüler et al. \(2019\)](#). The financial cycle indicator takes high values when total non-financial credit volumes grow at a fast pace, and real estate, equity, and bond prices grow at a fast pace as well. Shaded areas indicate CEPR euro area recession periods.



credit volumes grow at an unusually fast pace (proxying a credit boom), and *ii*) real estate, equity, and bond prices grow at an unusually fast pace as well *at the same time* (proxying asset price inflation). In this sense, their financial cycle indicator is not a measurement of credit growth, which can be beneficial, but of *bad*, or excess, credit growth that coincides with asset price inflation.

The financial cycle indicator is available for the euro area and the U.S. from the authors. Their indicator took high values during the dot-com boom years between 1997 and 2000, and during the credit boom years preceding the 2008–2009 global financial crisis. Their indicator took particularly low values in 2009 and 2011, times associated with crisis-induced fire sales and financial system deleveraging.

## 4 Empirical results

Our empirical study is structured around the following interrelated questions. Which variables other than real GDP growth should be included in a multivariate quantile model for downside risk measurement purposes? Do quantile regression estimates differ significantly across quantiles? How large were downside risks to the euro area economy stemming from financial stress and vulnerabilities? Is the euro area economy at all times equally vulnerable to a fixed sequence of adverse shocks? Does managing the financial cycle pay off in terms of less volatile macroeconomic outcomes? Finally, (when) does it pay off to adopt active macroprudential policies? We focus our discussion on the euro area, and report analogous tables and figures for U.S. data in [Web Appendix E](#).

### 4.1 Variable selection exercise

A two-variable QVAR model for quarterly real GDP growth and the CISS provides a minimal system to study downside risks to the real economy. GDP growth is required to quantify downside risks, and the CISS significantly impacts the left tail of the predictive GDP growth distribution; see [Section 4.2](#) below. This minimal system, however, may miss important interactions with other economic variables. In addition, it misses a variable that can be influenced directly through financial stability policies. This section presents the main results of a systematic search over potential additional endogenous variables to be included in a QVAR.

Our variable selection exercise is set up as follows. We estimate a recursive trivariate QVAR for  $\tilde{x}_t = (y_t, z_t, s_t)'$ , consisting of annualized quarterly real GDP growth  $y_t$ , a third variable  $z_t$  to be affected by macroprudential policies, and the CISS  $s_t$ . Sandwiching  $z_t$  between  $y_t$  and  $s_t$  implies that  $z_t$  can explain  $s_t$  (the CISS) both instantaneously and with a lag. We loop over many available macro-financial variables  $z_t$ . For each case we evaluate the average quantile regression objective function at quantiles ranging from 0.1 to 0.9 (decile-by-decile). The objective function is evaluated only for the GDP growth and CISS equations, as these variables remain fixed across loops.

Each trivariate system is estimated for the same number of data points and deterministic model parameters. As a result, information criteria penalty terms are the same across specifications, and can therefore be set to zero for model comparison purposes without loss of generality.<sup>16</sup>

Figure 2 presents our main variable selection results for the euro area. Variables are ranked in terms of average check function values – the smaller the better. Non-stationary time series are de-trended using [Hamilton \(2018\)](#)'s regression filter, and are marked with a star (\*) in the figure legend.

Two variables stand out as interacting closely with euro area GDP growth and financial stress at all nine quantiles. Both are related to central bank policy instruments. The de-trended three-months EURIBOR rate, a measure of monetary policy, is ranked first, impacting both future GDP growth as well as current financial conditions. [Schüler et al. \(2019\)](#)'s broad financial cycle indicator (see Section 3.3) is ranked second, followed by the euro area's capacity utilization rate. Capacity utilization is a business cycle indicator, and as such highly correlated with GDP growth, and arguably of lesser interest in a financial stability context.

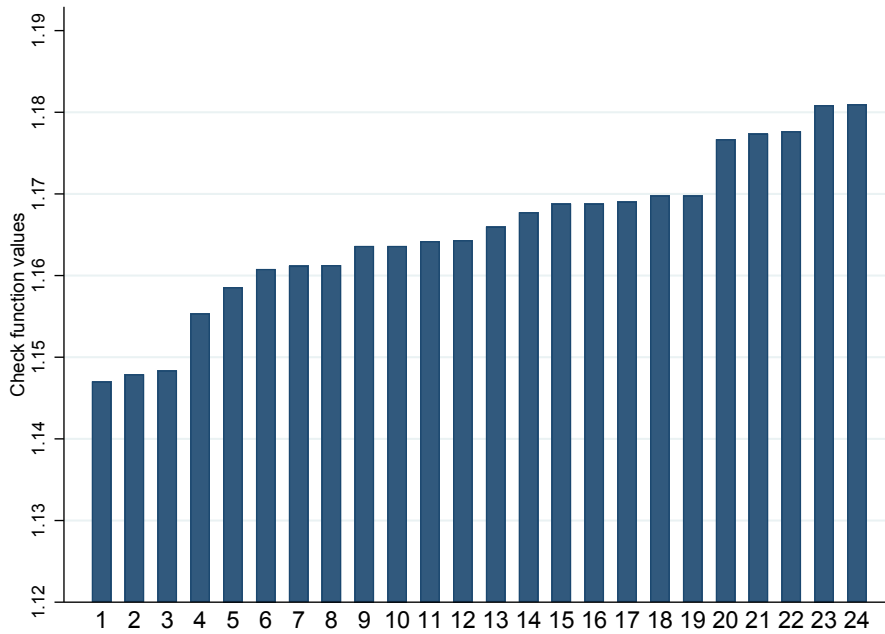
Web Appendix E.2 reports analogous results for U.S. data. Approximately similar variables are selected.

---

<sup>16</sup>For a discussion of model selection between different quantile time series models see e.g. [Lee et al. \(2014\)](#).

## Figure 2: Variable selection

Variables are ranked according to their average check function value in a three-variable QVAR. Real quarterly GDP growth and CISS are fixed variables in the QVAR. Check function variables are evaluated at quantiles from 0.1 to 0.9 (decile-by-decile) for US GDP growth and US CISS only. Estimation sample is 1976Q2 to 2018Q4. Non-stationary time series are de-trended using [Hamilton \(2018\)](#)'s regression filter and are indicated in the legend with an asterisk (\*).



- |   |  |
|---|--|
| 1 3-Month Euribor                                 | 2 Broad FinCycle Indicator*                                    |
| 3 Capacity Utilization Rate*                      | 4 Loans to Households (HHs) and Non-Profit Orgs Serving HHs    |
| 5 Systemic Risk Indicator (Mean), EA19*           | 6 Systemic Risk Indicator (Median), EA19*                      |
| 7 EURO STOXX 50 Price Index                       | 8 News-Based Economic Policy Uncertainty Index*                |
| 9 House Price Index-DPI Ratio, EA17               | 10 Standardised House Price Index-DPI Ratio, EA17              |
| 11 House Price Index, EA17                        | 12 10-Year US-Euro Area Interest Rate Spread                   |
| 13 House Price Index                              | 14 Narrow FinCycle Indicator                                   |
| 15 Standardised House Price Index-DPI Ratio       | 16 House Price Index-DPI Ratio                                 |
| 17 Current Account Balance as a Share of GDP*     | 18 Standardised House Price Index-Rent Price Index Ratio, EA17 |
| 19 House Price Index-Rent Price Index Ratio, EA17 | 20 Loans to Non-Financial Corporations                         |
| 21 Unemployment Rate*                             | 22 10-Year Government Bond Yield                               |
| 23 Total Employment                               | 24 Gross Household Saving Rate                                 |

## 4.2 Model specification and parameter estimates

We choose a trivariate QVAR specification as our benchmark model. Our benchmark model consists of annualized quarterly real GDP growth  $y_t$ , the financial cycle indicator  $c_t$ , and the CISS  $s_t$ . We therefore consider  $\tilde{x}_t = (y_t, c_t, s_t)'$ .

Figure 3 reports parameter and standard error estimates for our baseline specification. Parameter point estimates are obtained equation-by-equation via  $np$  univariate quantile regressions. The appropriate standard error bands about the parameter point estimates, however, do not coincide with the equation-by-equation estimates as supplied by common software packages. The standard errors reported in Figure 3 take cross-equation restrictions at common quantiles into account, see Web Appendix B.1 for details, and can be tighter or wider compared to the equation-by-equation standard error estimates.

We discuss the parameter estimates from top left to bottom right. Each of the panels presents the parameter estimates across nine deciles together with 95% confidence bands and the corresponding least squares estimate. The arrangement of panels in Figure 3 corresponds to the ordering of variables in (6). Overall, the quantile regression estimates differ substantially across quantiles, as well as from their least squares counterparts. Each intercept estimate in  $\omega$  increases monotonically in the considered quantile. This pattern is by construction, and reflects the fact that quantile shocks are not centered around zero; see (11).

All contemporaneous effects are visible from matrix  $A_0$ . The contemporaneous impact of GDP growth on the financial cycle (element [2,1]) as well as on the CISS (element [3,1]) is small and rarely statistically significant. The [3,2]-element of  $A_0$  points to a positive contemporaneous impact of the financial cycle on the CISS at its lower quantiles. This element is a mirror image of the [3,2]-element in  $A_1$ . Taken together, they suggest that the CISS is high when the the financial cycle falls (or vice versa). This is intuitive, as financial sector deleveraging and financial stress tend to go hand-in-hand.

All lagged effects are visible from matrix  $A_1$ . The [1,3]-element points to the familiar finding that the effect of financial stress (CISS) on future GDP growth is approximately zero at the upper

quantiles of future GDP growth, but markedly negative, and significantly different from zero, at its lower quantiles. As a result, a positive shock to the CISS (i.e., increased, or more widespread financial stress) shifts the lower tail of the predictive GDP distribution toward more negative values, while leaving its upper quantiles less affected. The [3,2]-element of  $A_1$  captures the lagged effect of the financial cycle on the CISS. The effect is positive and statistically significant, particularly for the CISS's upper quantiles. As a result, a positive shock to the financial cycle (e.g., an increasingly bad credit boom) at time  $t$  shifts the right tail of the CISS at  $t + 1$  towards more adverse values. Put differently, excessive (bad) credit growth increases the likelihood of elevated financial stress in the future.

The [3,3]-element of  $A_1$  captures the autoregressive coefficient associated with the CISS. The estimate exceeds one at the 0.9 quantile, pointing to a local non-stationarity in the rightmost tail. Local non-stationarity is not uncommon in QAR models, and does not imply global non-stationarity; see [Koenker \(2005, Ch. 8.3\)](#). Indeed, conditional quantiles simulated from our QVAR model at estimated parameters converge to their unconditional counterparts. The standard errors around the locally non-stationary estimate are, however, not reliable, and not reported for this reason.

Three specifications have been run for robustness. [Web Appendix D.1](#) studies a linear VAR for  $\tilde{x}_t$ . The downside risk estimates obtained from the linear VAR model are visibly different from those obtained from the QVAR model. The parameter homogeneity restrictions implied by the linear specification tend to be rejected; see [Section 4.3](#) below.

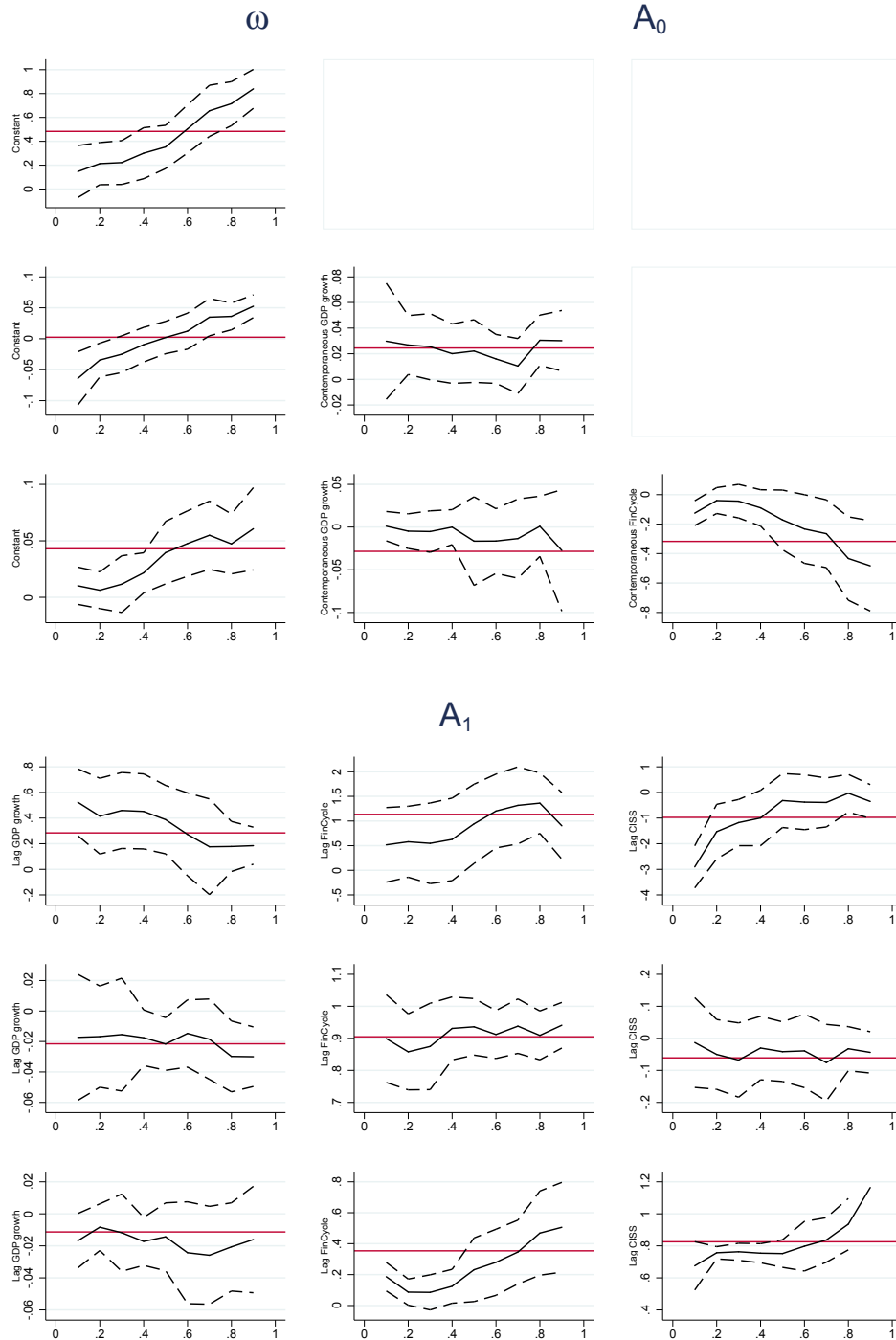
The variable selection exercise in [Section 4.1](#) suggested that short-term interbank rates can be a useful additional variable to consider in a QVAR. [Web Appendix D.2](#) studies a five-variable monetary structural QVAR model. This model additionally contains the three-month EURIBOR rate as well as quarterly changes in the GDP deflator (inflation). This monetary structural QVAR model is of considerable interest in its own right. It yields, however, broadly similar predictions in terms of downside risks and measures of macro-prudential policy stance. We therefore proceed with the above more parsimonious trivariate model for simplicity.

Web Appendix [D.3](#) extends our baseline model with an additional, annual lag for all variables. Information criteria prefer the more parsimonious version. Average future growth shortfall responds more quickly, and more severely, to contemporaneous financial stress when based on a single-lag specification. We therefore proceed with the single-lag specification.

Web Appendix [E.3](#) reports parameter and standard error estimates based on our baseline QVAR model for U.S. data. The parameter estimates are broadly in line with those for the euro area: Growing financial vulnerabilities shift the right tail of the U.S. CISS towards more positive values. A shock to the U.S. CISS shifts the left tail of the predictive GDP growth distribution towards more negative values, while leaving the right tail less affected.

**Figure 3: Parameter estimates for baseline QVAR model**

Parameter estimates from a trivariate QVAR model estimated for  $p = 9$  quantiles from 0.1 to 0.9. Variables are ordered GDP growth (respective first row), financial cycle (second row), and CISS (third row). Parameter estimates are obtained equation-by-equation while standard error estimates take cross-equation restrictions into account; see Web Appendix B.1. Standard error bands are dashed and at a 95% confidence level. Red horizontal lines indicate least squares estimates. Estimation sample is 1988Q3 to 2018Q4.



### 4.3 Wald test and quantile impulse response functions

Table 1 reports the outcome of three Wald  $\chi^2$  tests of parameter homogeneity across quantiles. We proceed equation by equation for  $i = 1, 2, 3$ . Each Wald test is implemented as explained in [Koenker \(2005, Ch. 3.3.2\)](#); see also [Koenker and Basset \(1982\)](#) and Web Appendix [B.2](#). The test rejects the parameter equality restrictions implied by a linear VAR for two of our three variables, GDP growth and CISS. Parameter homogeneity is most forcefully rejected for the GDP growth equation. The test outcomes are intuitive given the parameter and standard error estimates reported in Figure 3.

The asymmetries implied by the test outcome can be visualized via quantile impulse response function (IRF) estimates. We refer to [Chavleishvili and Manganelli \(2019\)](#) and Web Appendix [B.3](#) for details on IRF in a structural QVAR model context. Figure 4 plots the QIRFs associated with the parameter estimates reported in Figure 3. As expected, the real GDP response to a shock to the CISS depends markedly on the quantile of the predictive distribution. The 0.1 quantile respond much more strongly than the 0.9 quantile to the same shock. A shock to the financial cycle decreases the CISS in the short term, while raising it over the medium term. The 0.9 quantile responds more strongly to a positive shock than the 0.1 quantile, narrowing the predictive distribution of the CISS.

Web Appendix [E.4](#) discusses the analogous results for U.S. data. The Wald test outcomes and impulse response function estimates are qualitatively similar.

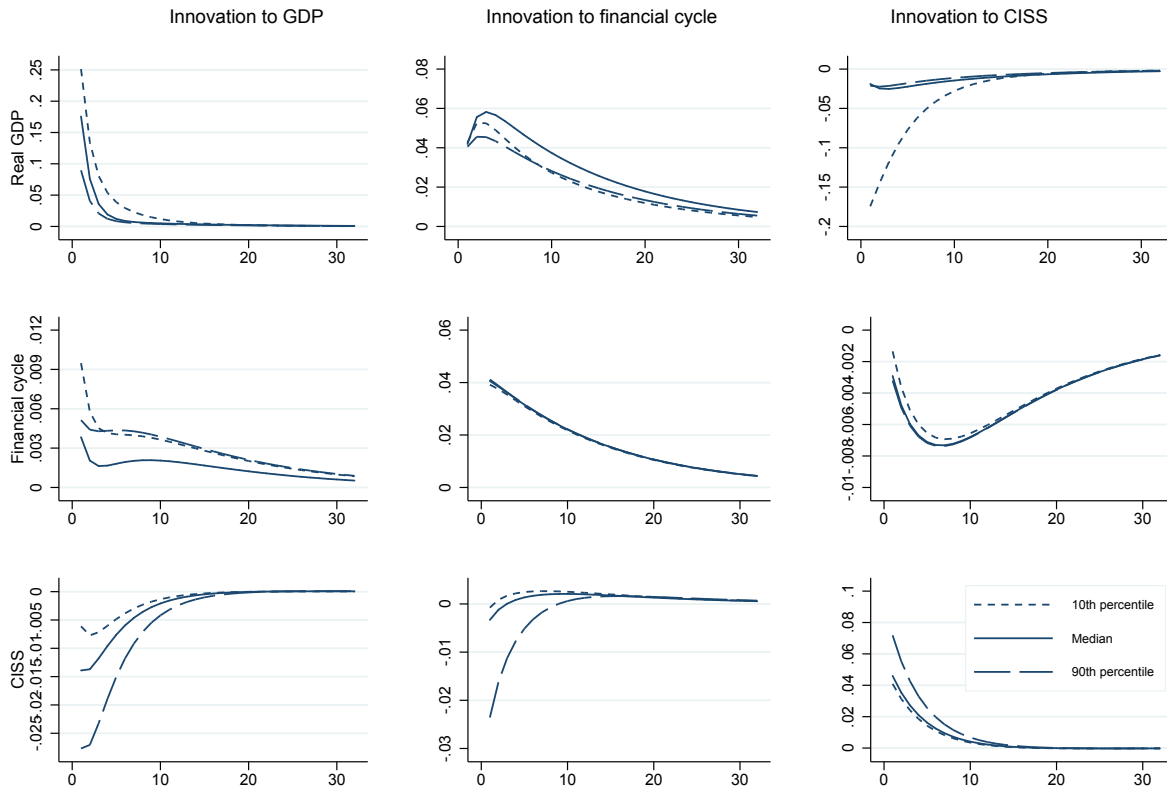
**Table 1: Wald test of parameter homogeneity.**

Wald tests statistics. The test's null hypothesis states that the quantile regression estimates, across  $p = 9$  quantiles, are equal to the median regression parameter estimates. We consider our baseline trivariate QVAR model, estimated decile-by-decile, ranging from 0.1 to 0.9; see Figure 3. The test statistic is  $\chi^2$ -distributed. The appropriate degrees-of-freedom (df) are given by the number of right-hand-side variables per equation (excluding the constant, 3, 4, and 5, respectively), times the number of imposed restrictions ( $9 - 1 = 8$ ).

	df	test statistic	p-value
real GDP growth, $y_t$	24	209.71	0.00
financial cycle indicator, $c_t$	32	26.12	0.76
CISS Financial stress index, $s_t$	40	79.52	0.00

**Figure 4: Quantile impulse response functions**

Impulse response functions implied by the parameter estimates reported in Figure 3. Variables are ordered as GDP growth (respective first row), financial cycle (second row), and CISS (third row). Estimation sample is 1988Q3 to 2018Q4.



## 4.4 Average future growth shortfall

This section discusses our downside risk estimates as introduced in Section 2.1. Figure 5 plots the average future growth shortfall (AGS) and longrise (AGL) for the euro area. The risk estimates are based on full-sample parameter estimates, but are otherwise conditional on variables observed up to time  $t$  only. Growth shortfall and longrise are forward-looking, and averaged over  $t + 1$  and  $t + 8$ ; see (3) and (5). To study the importance of including current financial conditions and medium-term vulnerabilities we compare our baseline QVAR model to a much simpler, univariate quantile autoregressive (QAR) model for GDP growth only. The QAR model does not include the financial cycle nor the CISS.

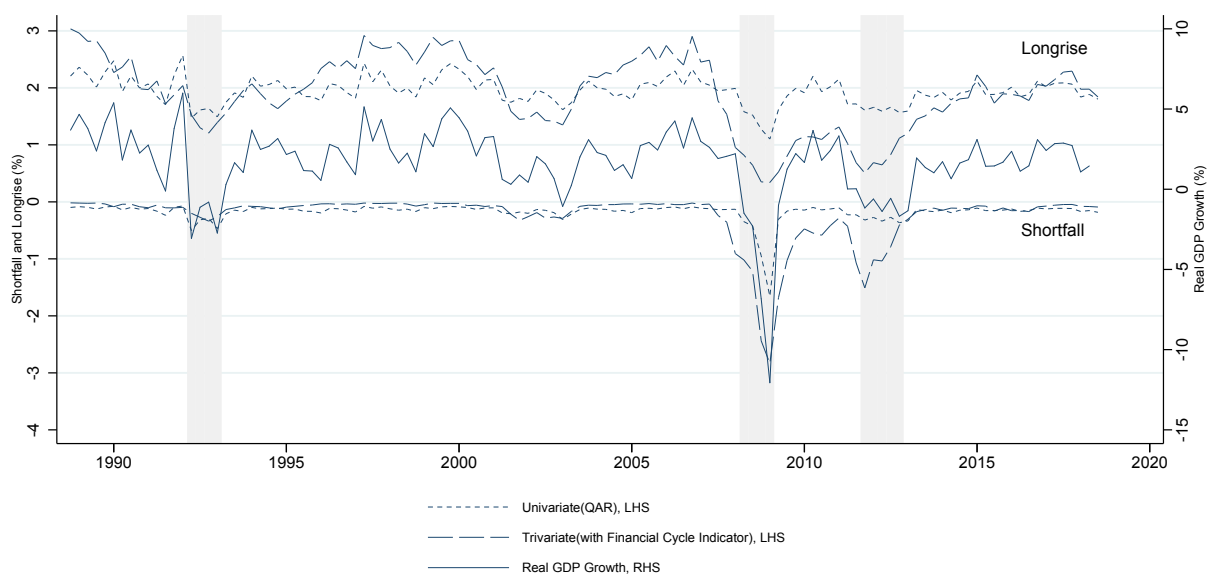
We focus on three findings. First, accounting for financial conditions is crucial. There is a pronounced difference between the downside risk (AGS) estimate implied by the trivariate QVAR and the univariate QAR. During the global financial crisis (GFC) between 2008 and 2009, the QAR-based downside risk estimate declines much later, and by much less, compared to the QVAR-based estimate. The sovereign debt crisis between 2010 and 2012 is missed almost entirely based on the QAR model.

Second, as a result of macro-financial interactions, the QVAR's lower quantiles for future GDP growth are more volatile than its upper quantiles. This observation mirrors those of [Adrian et al. \(2020\)](#), who focus on single quantiles in isolation. Web Appendix D.5 plots the tail conditional expectation and expected probability of a contraction underlying  $GS_{t,t+1:t+H}^{\tau}$  and  $GL_{t,t+1:t+H}^{\tau}$  separately; see the first and second term in (2) and (4), respectively. Most of the variability in  $AGS_{t,t+1:t+8}^{\tau}$  comes from the changes in growth conditional on being in a recession-term, with an additional contribution from increasing the probability of a contraction in bad times.

Lastly, the downside risks implied by the QVAR model can be economically large. The GFC implied an extreme AGS over eight quarters of approximately -3.5%. This corresponds to a  $(1 - 0.035/4)^8 - 1 \approx -6.8\%$  reduction in real living standards. This is a substantial expected contraction, reflecting severe downside risks from a deterioration of financial conditions. During median times, the estimated AGS is approximately -0.5% and corresponds to a more moderate risk

**Figure 5: Euro area AGS and AGL estimates**

Time- $t$  average future growth shortfall ( $AGS_{t,t+1:t+8}^{\tau}$ ) and average future growth longrise ( $AGL_{t,t+1:t+8}^{\tau}$ ) estimates evaluated at  $\tau = 0$ ; see (3) and (5). The trivariate estimate is based on our baseline QVAR model (dashed line, scale on left axis) that allows for macro-financial interactions. The univariate estimate is based on a one-equation restricted model with a constant and lagged GDP growth as the only right-hand-side variables (dotted line, scale on left axis). Each model is estimated for  $p = 20$  quantiles ranging from 0.025 to 0.975. We compare these estimates to quarterly annualized real GDP growth (solid line, scale on right axis). Shaded areas indicate euro area recessions as determined by the CEPR business cycle dating committee. The estimation sample is 1988Q3 to 2018Q4.



of a  $(1 - 0.005/4)^8 - 1 \approx -1.0\%$  reduction in real living standards.

From a risk management perspective the AGS can be compared to the AGL as the latter provides an indication of the upside for the economy. The GFC did not only generate an extremely low value for the AGS, but also for the AGL. With a value of only 0.4%, the average expected expansion of the economy over the following eight quarters would have been approximately 0.8%. This compares to an average of approximately 4% over the entire sample. The GFC thus reduced living standards especially because of the contraction, but also persistently muted the upside potential of the economy, and did so until early 2015.

Web Appendix E.5 discusses the analogous figure for U.S. data. Similar observations hold true for these data as well: Accounting for financial conditions is crucial. Model-implied lower

quantiles for future GDP growth are more volatile than upper quantiles. Downside risks vary substantially over time and can be economically large.

## 4.5 Model-based stress testing

Our structural QVAR model provides a natural environment to perform model-based stress testing exercises. We here understand stress testing as a forecast of what would happen to  $\tilde{x}_t$  conditional on the system being subjected to a certain fixed sequence of adverse shocks. We refer to such a sequence of adverse shocks as a stress scenario. For the computation of forecasts conditional on such scenarios we refer to Section 2.5. Our stress testing approach is different from supervisory stress tests in that our main variable of interest is not banking sector health but real economic (GDP) impact.

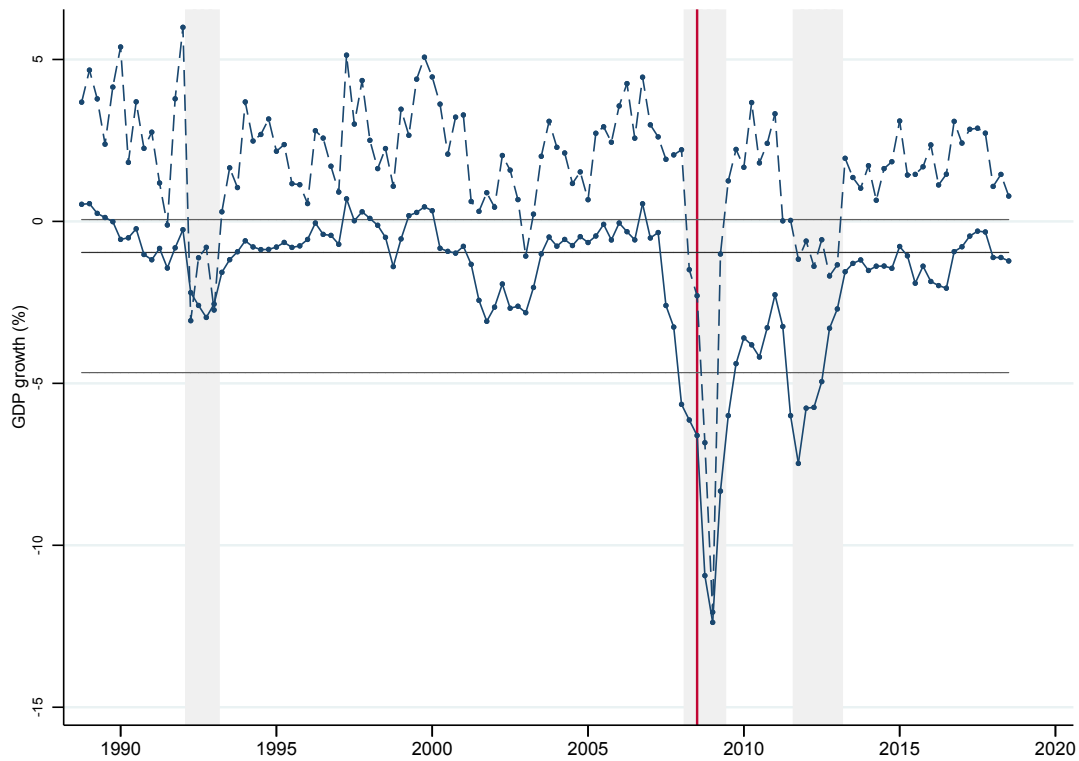
Figure 6 reports the time- $t$  conditional forecast of average future real GDP growth  $\hat{y}_{t,t+1:t+8}$  between time  $t$  and  $t + 8$  as implied by our trivariate model. The forecast is conditional on a 0.1 (conditional) quantile realization for GDP growth  $y_{t+h}$ , a 0.1 quantile realization of the financial cycle  $c_{t+h}$ , and a 0.8 quantile realization for CISS  $s_{t+h}$ , consecutively for  $h = 1, \dots, 8$ . The magnitude of these shocks is approximately in line with the eight observed quantile realizations for all variables between 2008Q1 and 2009Q4. The stress test is repeated at each  $t = 1, \dots, T$ , and always based on the same (full sample) parameter estimates. As a result, the figure is informative about the impact of GFC-sized real and financial shocks on real living standards at any time in our sample.

We observe that the euro area economy is not equally resilient to the same stress scenario at all times. This is a direct consequence of the asymmetries (nonlinearities) inherent in the estimated QVAR model. When financial imbalances and financial stress are high, real GDP growth is particularly vulnerable.

Figure 6 can be informative when assessing macro-prudential policy stance. An unusually high level of vulnerability to future real and financial shocks — a value of  $\hat{y}_{t,t+1:t+8}$  below its own 10% quantile, say — indicates that large shocks have materialized and macro-prudential buffers

**Figure 6: Vulnerability to GFC-sized shocks**

Dashed line: euro area annualized quarterly real GDP growth. Solid line: predicted average annualized quarterly real GDP growth  $\hat{y}_{t,t+1:t+8}$  two years ahead conditional on consecutive 0.1 quantile realizations for GDP growth  $y_t$ , 0.1 quantile realizations of the financial cycle  $c_t$ , and 0.8 quantile realizations for CISS  $s_t$ . Predictions are based on full sample parameter estimates. Estimations sample 1988Q3 – 2018Q4. Horizontal lines refer to 0.1, 0.5, and 0.9 empirical quantiles of  $\hat{y}_{t,t+1:t+8}$ .



should be released. In the euro area, such values are observed during the financial crisis of 2008 – 2009 and the sovereign debt crisis in 2011 – 2012. Low to moderate levels of vulnerability indicate times when macro-prudential buffers could be built up. Gradually growing macro-prudential capital buffers help increase banking sector resilience, lean against bad credit growth, improve incentives, and are available to be released later whenever necessary.

Web Appendix E.6 discusses the analogous figure for U.S. data. Similar observations hold true for these data as well.

## 4.6 The benefits from active macroprudential policy

An active debate in policy circles and academia revolves around the question which policies should be used to address financial stability risks. Should macro-prudential policy be the first line of defense? Or should monetary policy be used instead to lean against the buildup of financial vulnerabilities?

To inform this debate this section proposes a thought experiment. We ask the question what would euro area real GDP growth have been had an all-powerful policy-maker been able to reset the financial cycle to its conditional median over the entire sample period, while leaving the structural shocks to the other variables unchanged. To interpret the outcome we need to assume that all quantile-specific parameters remain fixed at their full-sample estimates as the system is subjected to counterfactual shocks.<sup>17</sup>

The counterfactual realizations are constructed as follows. At any time  $t = 1, \dots, T$ , given a counterfactual realization  $\hat{x}_{i,t}$ , there are  $p$  potential paths for variable  $i$  to go down to arrive at  $\hat{x}_{i,t+1}$ . For any variable  $i$  other than the financial cycle, we select the path corresponding to the filtered structural shocks. For the financial cycle we always select the conditional median path. Given  $\hat{x}_{t+1}$ , we repeat the procedure for all  $t$ .

The top left, top right, and bottom left panels in Figure 7 compare real-world data with counterfactual model-based outcomes for real GDP growth, financial cycle, and financial stress in the euro area. The final bottom-right panel presents Kernel estimates of the distribution of real GDP growth in either case. We find that leaning against the financial cycle is not obviously costly in terms of expected growth. In fact, expected growth is *higher* in the counterfactual scenario as it increases from 1.66% to 1.83% annualized real GDP growth. In addition, economic growth is more stable (less volatile around its mean) and less skewed to the downside in the counterfactual scenario.

Table 2 reports descriptive statistics for the real-world GDP growth sample (left column) and its counterfactual counterpart (right column). Extremely negative and extremely positive realizations

---

<sup>17</sup>This assumption can be phrased and tested in terms of the “super-exogeneity” of certain variables; see Engle et al. (1983) and Favero and Hendry (1992). Accordingly, the policy interventions should be small enough to not cause pronounced variation in deterministic parameters; see e.g. Lucas (1976).

for GDP growth disappear from the counterfactual sample. Both mean and median growth are higher, volatility is lower, and growth is less skewed to the downside in the counterfactual sample. These findings are in line with e.g. [Brandao-Marques et al. \(2020\)](#), who find that macro-prudential policies are effective in dampening downside risks to economic growth stemming from the build-up of financial vulnerabilities. In addition, our results suggest that policy makers can lean against financial vulnerabilities at little-to-no cost to mean (trend, potential) GDP growth.

The objective function (18) can be used to study the welfare benefit associated with managing the financial cycle. We evaluate

$$u_t(\text{Scenario}) = \sum_{h=1}^{12} \bar{\hat{y}}_{t,t+h}(\text{Scenario}) + 0.25 \cdot \widehat{\text{GS}}_{t,t+h}(\text{Scenario}), \quad (19)$$

where  $\bar{\hat{y}}_{t,t+h}$  is the average taken over  $p$  realizations of  $\hat{y}_{t,t+h}$ , parameters are chosen as  $\beta = 1$ ,  $\lambda = 1.25$ , and  $\tau = 0$ , and where we truncated the infinite sum after  $H = 12$ . One reason to penalize downside risks to the economy is that they can change the expected future growth path of the economy; see [Section 4.4](#).

[Figure 8](#) plots the utility difference  $\Delta u_t = u_t(\text{active}) - u_t(\text{passive})$  associated with adopting the active macro-prudential policy. Adopting a less-passive financial stability policy is not equally beneficial at all times. The benefits from leaning against bad credit growth are maximal during the late 1980s around the fall of the iron curtain in some European countries before the 1992 recession, during the late 1990s before the bust of the dot-com boom in 2000, and during the mid-2000s before the onset of the global financial crisis in 2007. The benefits from leaning against the financial cycle are estimated to be negative following the global financial crisis in 2009, and following the euro area sovereign debt crisis in 2012. This is intuitive, as the financial system was already deleveraging during these times, and requiring more would add insult to injury. The utility difference  $\Delta u_t$  is strongly correlated with the euro area financial cycle, suggesting that it is a valuable variable to track to inform macroprudential policy discussions.

[Web Appendix E.7](#) reports the corresponding figure and table for U.S. data. Both mean and

median are higher in the counterfactual sample of a managed financial cycle. Adopting an active financial stability policy is not equally beneficial at all times.  $\Delta u_t$  is less strongly associated with the financial cycle in the U.S. than in the euro area.

### Figure 7: Leaning against the financial cycle

Top left panel: actual quarterly annualized real GDP growth for the euro area, and counterfactual data assuming that the policy maker resets the financial cycle to its conditional median at all times. Top right panel: actual and counterfactual values for the financial cycle. Bottom left panel: actual and counterfactual values for financial stress. Bottom right panel: Kernel estimate over a histogram of actual and counterfactual real GDP growth. Actual data are in solid lines. Counterfactual realizations are in dashed lines.

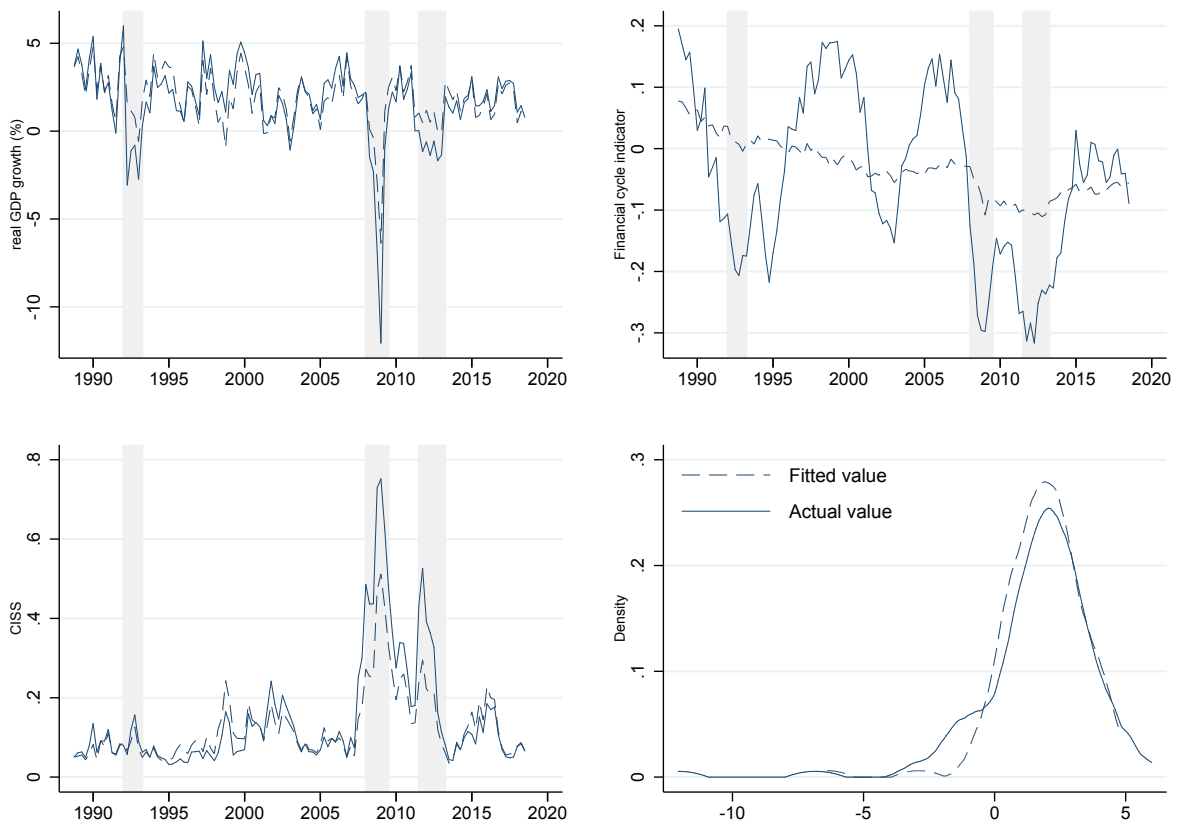


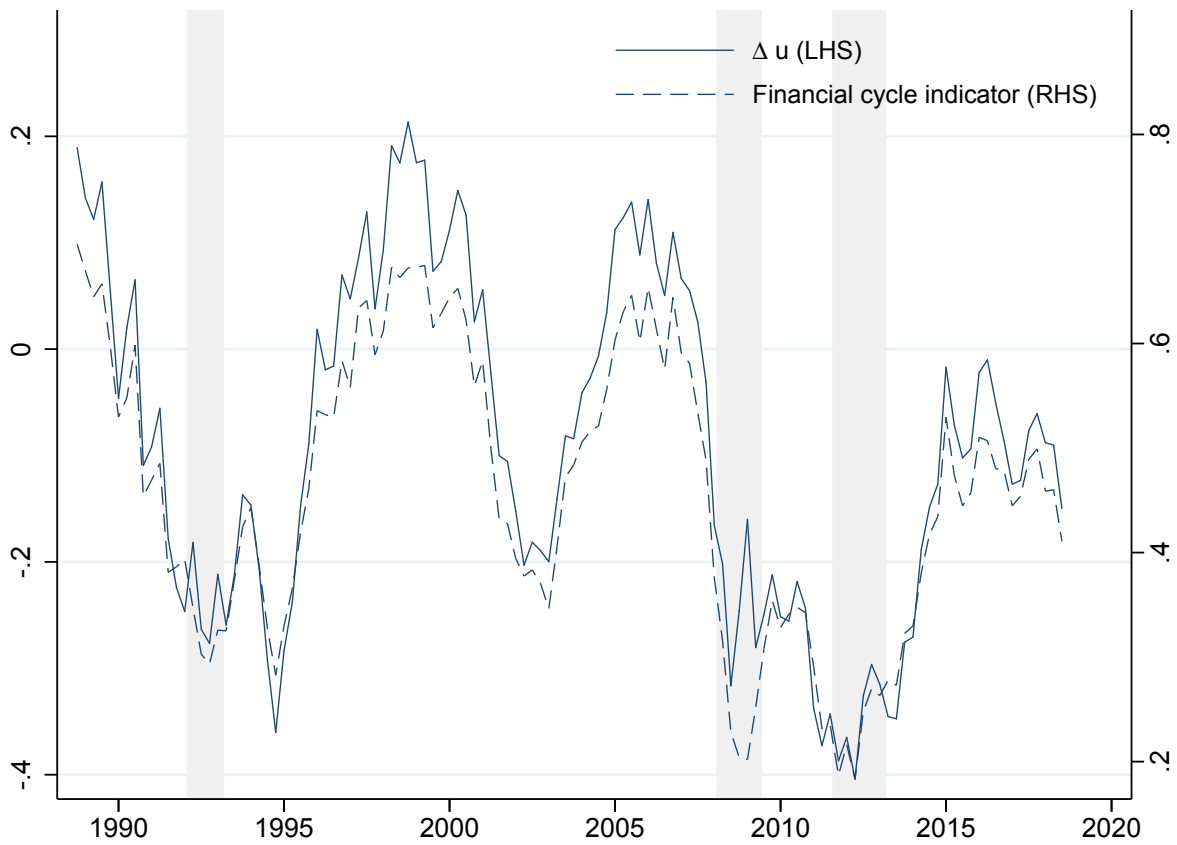
**Table 2: Comparison actual vs. counterfactual euro area growth rates**

Left column: actual quarterly annualized real GDP growth for the euro area. Right column: counterfactual data assuming that a policy maker could reset the financial cycle to its median conditional value at any time. Estimation sample is 1988Q3 to 2018Q4.

	Real GDP growth	Counterfactual GDP growth
Moments		
Mean	1.664	1.830
Std. Dev.	2.275	1.559
Variance	5.175	2.431
Skewness	-2.331	-1.311
Kurtosis	13.929	8.509
Percentiles		
1%	-6.831	-2.901
5%	-1.587	-.299
10%	-1.039	.131
50%	1.980	1.885
90%	3.785	3.707
95%	4.456	4.236
99%	5.386	4.822
Smallest values		
1st	-12.065	-6.393
2nd	-6.831	-2.901
3rd	-3.065	-1.313
4th	-2.735	-.796
Largest values		
4th	5.070	4.369
3rd	5.134	4.424
2nd	5.386	4.822
1st	5.993	4.829

**Figure 8: The benefits from active macro-prudential policy**

The benefit of adopting an active macro-prudential policy stance in utility terms,  $\Delta u_t = u_t(\text{active}) - u_t(\text{passive})$ ; see (19). Parameters are chosen as  $\beta = 1$ ,  $\lambda = 1.25$ ,  $\tau = 0$ , and  $H = 12$ . The difference is based on full sample estimates. Estimation sample is 1988Q3 to 2018Q4. Shaded areas indicate euro area recessions.



## 5 Conclusion

We proposed a structural QVAR model that relates downside risks to the economy to measures of financial stress and medium-term vulnerabilities. In an empirical study of euro area and U.S. data between 1988Q3 and 2018Q4 we found that the dynamic properties of the system differ across quantiles. The left quantiles of the predictive GDP growth distribution is related to a contemporaneous indicator of systemic stress, whose right quantiles are related to financial vulnerabilities. Counterfactual simulations allow us to construct urgently-needed indicators of macro-prudential policy stance, and to assess when macro-prudential interventions are relatively more likely to be beneficial.

## References

- Adrian, T., J. Berrospide, S. Chavleishvili, R. Lafarguette, and S. Manganelli (2020). Macro stress testing for banks. *mimeo*.
- Adrian, T., N. Boyarchenko, and D. Giannone (2020). Multimodality in macro-financial dynamics. *NY Fed staff reports 903*, 1–54.
- Adrian, T., F. Grinberg, N. Liang, and S. Malik (2018). The term structure of growth-at-risk. *IMF working paper*.
- Aikman, D., J. Bridges, S. H. Hoke, C. O’Neill, and A. Raja (2019). Credit, capital and crisis: a GDP-at-risk approach. *Bank of England working paper 824*.
- Almon, S. (1965). The distributed lag between capital appropriations and net expenditures. *Econometrica 33*, 178–196.
- Artzner, P., F. Delbaen, J. M. Eber, and D. Heath (1999). Coherent measures of risk. *Mathematical Finance 9(3)*, 203–228.
- Beutel, J. (2019). Forecasting growth at risk. *mimeo*.

- Bianchi, J. (2011). Overborrowing and systemic externalities in the business cycle. *American Economic Review* 101, 34003426.
- Brandao-Marques, L., G. Gelos, M. Narita, and E. Nier (2020). Leaning against the wind: An empirical cost-benefit analysis. *IMF working paper*, 1–54.
- Brownlees, C. and A. B. M. Souza (2019). Backtesting global growth-at-risk. *UPF working paper*.
- Caldara, D., C. Scotti, and M. Zhong (2019). Macroeconomic and financial risks: A tale of volatility. *mimeo*.
- Carney, M. (2020). The grand unifying theory (and practice) of macroprudential policy. *Speech given at University College London on 5 March 2020*, 1 – 22.
- Carriero, A., T. E. Clark, and M. Marcellino (2020). Capturing macroeconomic tail risks with Bayesian vector autoregressions. *working paper 2020*, 1–68.
- Chavleishvili, S. and S. Manganelli (2019). Forecasting and stress testing with quantile vector autoregression. *ECB working paper 2330*, 1 – 43.
- Duprey, T. and A. Ueberfeldt (2020). Managing GDP tail risk. *Bank of Canada working paper 2020–03*, 1–63.
- ECB (2019). European Central Bank Financial Stability Review, May 2019. .
- Engle, R. F., D. F. Hendry, and J.-F. Richard (1983). Exogeneity. *Econometrics* 51(2), 277 – 304.
- Fagan, G., J. Henry, and R. Mestre (2001). An area-wide model (AWM) for the euro area. *ECB working paper 42*.
- Favero, C. and F. D. Hendry (1992). Testing the lucas critique: A review. *Econometric Reviews* 11(3), 265–306.
- Fishburn, P. (1977). Mean-risk analysis with risk associated with below-target returns. *American Economic Review* 67, 116–126.

- FSB (2009). Report to G20 Finance ministers and governors: Guidance to assess the systemic importance of financial institutions, markets and instruments – initial considerations. *www.fsb.org*.
- Gilchrist, S. and E. Zakrajsek (2012). Credit spreads and business cycle fluctuations. *American Economic Review* 102(4), 1692–1720.
- Hahn, J. (1995). Bootstrapping quantile regression estimators. *Econometric Theory* 11(1), 105–121.
- Hamilton, J. D. (2018). Why you should never use the Hodrick-Prescott filter. *Review of Economics and Statistics* 100, 831–843.
- He, Z. and A. Krishnamurthy (2019). A macroeconomic framework for quantifying systemic risk. *American Economic Journal: Macroeconomics* 11(4), 1 – 37.
- Hollo, D., M. Kremer, and M. L. Duca (2012). CISS – A composite indicator of systemic stress in the financial system. *ECB Working Paper 1426*.
- IMF (2017). Global financial stability report: Is growth at risk? *IMF Global Financial Stability Report 3*, 91–118.
- Koenker, R. (2005). *Quantile Regression*. Cambridge: Cambridge University Press.
- Koenker, R. and G. Basset (1982). Robust tests for heteroscedasticity based on regression quantiles. *Econometrica* 50, 43 – 61.
- Koopman, S. J. and J. D. Durbin (2000). Fast filtering and smoothing for multivariate state space models. *Journal of Time Series Analysis* 21, 281–296.
- Koyck, L. M. (1954). *Distributed lags and investment analysis*. North-Holland, Amsterdam.
- Lee, E. R., H. Noh, and B. U. Park (2014). Model selection via Bayesian Information Criterion for quantile regression models. *Journal of the American Statistical Association* 109(505), 216–229.
- Lucas, R. (1976). Econometric policy evaluation: A critique. In K. Brunner and A. Meltzer (Eds.), *The Phillips Curve and labor markets* (1 ed.), pp. 19–46. New York: Carnegie-Rochester conference series on public policy, American Elsevier.

- Manganelli, S. and L. Kilian (2008). The central banker as a risk manager: Estimating the Federal Reserves preferences under Greenspan. *Journal of Money, Credit, and Banking* 40, 1103–1129.
- McNeil, A., R. Frey, and P. Embrechts (2005). *Quantitative Risk Management*. Princeton: Princeton University Press.
- Prasad, A., S. Elekdag, P. Jeasakul, R. Lafarguette, A. Alter, A. F. Xiaochen, and C. Wang (2019). Growth at risk: Concept and applications in IMF country surveillance. *IMF working paper*.
- Schüler, Y., P. Hiebert, and T. A. Peltonen (2019). Financial cycles: Characterisation and real-time measurement. *Journal of International Money and Finance*, forthcoming.
- Sims, C. A. (1980). Macroeconomics and reality. *Econometrica* 48, 148.
- Svensson, L. E. (2017). Leaning against the wind: the role of different assumptions about the costs. *NBER Working Paper 23745*, 1 – 53.

Web Appendix to  
The risk management approach  
to macro-prudential policy\*

*Sulkhan Chavleishvili,<sup>(a)</sup> Robert F. Engle,<sup>(b)</sup> Stephan Fahr,<sup>(a)</sup>  
Manfred Kremer,<sup>(a)</sup> Simone Manganelli,<sup>(a)</sup> Bernd Schwaab<sup>(a)</sup>*

<sup>(a)</sup> European Central Bank, Financial Research,

<sup>(b)</sup> New York University Stern School of Business

**\*\*\* preliminary \*\*\***

---

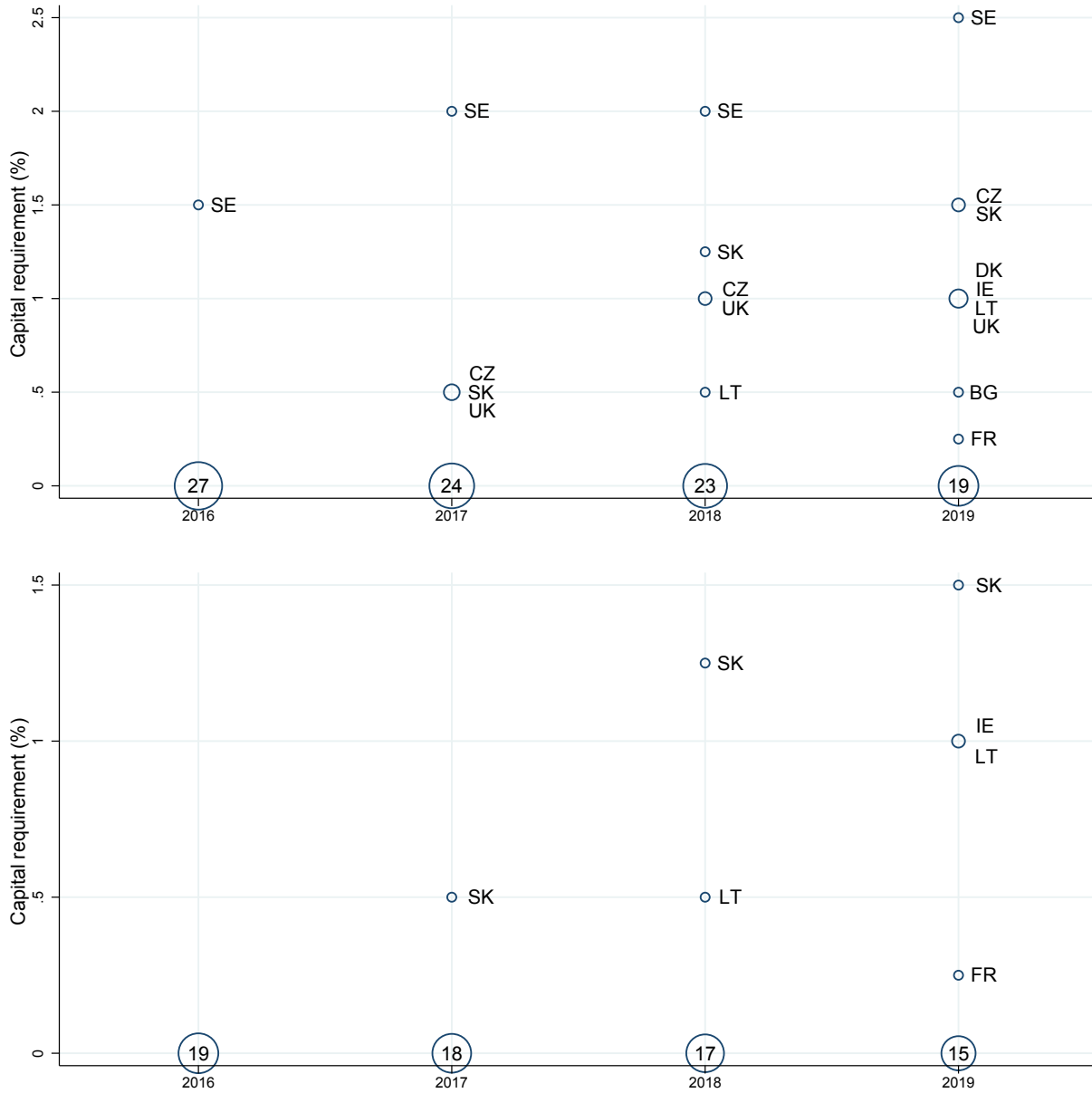
\*E-mail contacts: [sulkhan.chavleishvili@ecb.int](mailto:sulkhan.chavleishvili@ecb.int); [rengle@stern.nyu.edu](mailto:rengle@stern.nyu.edu); [stephan.fahr@ecb.int](mailto:stephan.fahr@ecb.int); [manfred.kremer@ecb.int](mailto:manfred.kremer@ecb.int); [simone.manganelli@ecb.int](mailto:simone.manganelli@ecb.int); [bernd.schwaab@ecb.int](mailto:bernd.schwaab@ecb.int). The views expressed in this paper are those of the authors and they do not necessarily reflect the views or policies of the European Central Bank.

## **A The non-cyclical nature of the counter-cyclical capital buffer**

Figure [A.1](#) plots the evolution of required counter-cyclical capital buffers (CCyB) for banks located in 28 European Union countries (top panel) and 19 euro area countries (bottom panel) between 2014 and 2019. By December 2019, five years after the introduction of CCyB, less than one in three countries have moved to positive CCyBs. The majority of countries have not activated this financial stability tool, in line with a potential inactivity bias.

### Figure A.1: The non-cyclical nature of the counter-cyclical capital buffer

Required counter-cyclical capital buffers for banks located in 28 European Union countries (top panel) and 19 euro area countries (bottom panel) between 2014 and 2019. The size of the circles is proportional to the number of countries for which the CCyB takes a certain value. Source: end-of-year data from the European Systemic Risk Board.



## B Technical details

### B.1 Parameter estimation and standard errors

The recursive QVAR model (10) – (11) can be estimated using the framework developed by White et al. (2015). Let  $q_t^\theta(\beta) \equiv \omega^\theta + A_0^\theta Y_t + A_1^\theta Y_{t-1}$  and  $q_{it}^{\theta_j}(\beta)$  the  $j^{\text{th}}$  quantile of the  $i^{\text{th}}$  variable of the vector  $q_t^\theta(\beta)$ , where we have made explicit the dependence on  $\beta$ , the vector containing all the unknown parameters in  $\omega^\theta$ ,  $A_0^\theta$ , and  $A_1^\theta$ . Define the quasi-maximum likelihood estimator  $\hat{\beta}$  as the solution of the optimization problem:

$$\hat{\beta} = \arg \min_{\beta} T^{-1} \sum_{t=1}^T \left\{ \sum_{i=1}^n \sum_{j=1}^p \rho_{\theta} \left( \tilde{Y}_{it} - q_{it}^{\theta_j}(\beta) \right) \right\}, \quad (\text{B.1})$$

where  $\rho_{\theta}(u) \equiv u(\theta - I(u < 0))$  is the standard check function of quantile regressions. The asymptotic distribution of the regression quantile estimator is provided by White et al. (2015), which we report here for convenience.

Under the assumptions of Theorems 1 and 2 of White et al. (2015),  $\hat{\beta}$  is consistent and asymptotically normally distributed. The asymptotic distribution is:

$$\sqrt{T}(\hat{\beta} - \beta^*) \xrightarrow{d} N(0, Q^{-1}VQ^{-1}) \quad (\text{B.2})$$

where

$$\begin{aligned} Q &\equiv \sum_{i=1}^n \sum_{j=1}^p E[f_{it}^{\theta_j}(0) \nabla q_{it}^{\theta_j}(\beta^*) \nabla' q_{it}^{\theta_j}(\beta^*)] \\ V &\equiv E[\eta_t \eta_t'] \\ \eta_t &\equiv \sum_{i=1}^n \sum_{j=1}^p \nabla q_{it}^{\theta_j}(\beta^*) \psi^{\theta_j}(\epsilon_{it}^{\theta_j}) \\ \psi^{\theta_j}(\epsilon_{it}^{\theta_j}) &\equiv \theta_j - I(\epsilon_{it}^{\theta_j} \leq 0) \\ \epsilon_{it}^{\theta_j} &\equiv \tilde{Y}_{it} - q_{it}^{\theta_j}(\beta^*) \end{aligned}$$

and  $f_{it}^{\theta_j}(0)$  is the conditional density function of  $\epsilon_{it}^{\theta_j}$  evaluated at 0.

The asymptotic variance-covariance matrix can be consistently estimated as suggested in Theorems 3 and 4 of [White et al. \(2015\)](#), or using bootstrap-based methods following [Buchinsky \(1995\)](#). Modern statistical softwares typically contain packages for quantile regression estimation and inference that estimate the above quantities. Our paper uses the interior point algorithm discussed by [Koenker and Park \(1996\)](#) and as implemented in Stata.

## B.2 Wald test for slope parameter homogeneity

The classical theory of linear regression *assumes* that the conditional quantile functions of the response variable given covariates are all parallel to one another. In our model, linearity implies that the slope parameters  $A_{0,i}^\gamma, A_{1,i}^\gamma$  (i.e. parameters other than the constant  $\omega_i$ ),  $i = 1, \dots, n$ , associated with different  $\gamma$ s are identical across  $\gamma$ s. Covariates effects then shift the location of the response distribution but do not change its scale or shape. In many applications, however, quantile regression parameter estimates often vary considerably across quantiles. As a result, an immediate and fundamental problem of inference in QR models involves testing for equality of slope parameters across quantiles. We proceed equation by equation for  $i = 1, 2, 3$ . The Wald test is implemented as explained in [Koenker \(2005, Ch. 3.3.2\)](#); see also [Koenker and Basset \(1982\)](#).

## B.3 Impulse response functions

Impulse response functions (IRFs) from our structural QVAR model can be defined in different ways, and each way has its advantages and drawbacks. This section derives IRFs that are closely related to standard IRFs from linear VAR models, facilitating their interpretation. For example, we can track the conditional median response of each variable instead of the conditional mean response. When median dynamics are used to propagate the initial shock, the signs of the off-diagonal parameters in  $A_0$  are of no concern; see footnote 11 in the main text.

## B.4 Simulation algorithm for downside risk measures

Let  $t = 1, \dots, T$  denote any time in our sample. We obtain time- $t$  conditional downside risk measures by simulating forward  $S = 10,000$  potential future paths for all  $n$  variables in  $\tilde{x}_{i,t+h}$ ,  $h = 1, \dots, 8$  quarters ahead.

We proceed as follows.

1. Fix any  $t = 1, \dots, T$ . Obtain and save full-sample parameter estimates for all variables at all  $p = 20$  quantiles  $0 < 0.025, 0.075, \dots, 0.925, 0.975 < 1$ . Set  $s = h = 1$ .
2. Draw  $n$  standard uniform random variables  $u_{i,t+h}$ , one for each variable  $1, \dots, n$ . Select variable-specific quantiles  $\gamma_{i,t+h}$  that are closest to  $u_{i,t+h}$ , respectively. Combine the chosen rows  $\omega_i^{\gamma_{i,t+h}}$ ,  $A_{0,i}^{\gamma_{i,t+h}}$ ,  $A_{1,i}^{\gamma_{i,t+h}}$  into QVAR parameter matrices  $\omega^\gamma$ ,  $A_0^\gamma$ ,  $A_1^\gamma$ .
3. Predict  $x_{t+h}$  one-step ahead using (6); see also (16).
4. Compute and save downside risk estimates  $\text{GS}_{t,t+h}^\tau$  and  $\text{GL}_{t,t+h}^\tau$  by evaluating the sample analogues of (2) and (4). For example,

$$\text{GS}_{t,t+h}^{\tau,(s)} = \tilde{x}_{1,t+h}^{(s)} \cdot 1\{\tilde{x}_{1,t+h}^{(s)} < \tau\},$$

where  $\tilde{x}_{1,t+h}^{(s)}$  denotes a simulated value for quarterly real GDP growth at time  $t + h$ .

5. If  $h < H$ , set  $h = h + 1$  and return to step 2. If  $h = H$ , compute  $\text{AGS}_{t,t+1:t+h}^\tau$  and  $\text{AGL}_{t,t+1:t+h}^\tau$  by averaging over  $\text{GS}_{t,t+h}^\tau$  and  $\text{GL}_{t,t+h}^\tau$ . Save these simulation-specific risk estimates.
6. If  $s < S$ , increase  $s = s + 1$  and return to step 2. If  $s = S$ , compute final time- $t$  downside risk measures as averages across simulation runs.

## C Data details

### C.1 CISS: construction details and data sources

The Composite Indicator of Systemic Stress (CISS) belongs to the family of financial stress indices (FSIs). FSIs are generally designed to quantify the level of stress in the whole or parts of the financial system. They do this by aggregating a certain number of individual stress indicators into a single statistic; see [Illing and Liu \(2006\)](#) and [Kliesen et al. \(2012\)](#) for surveys. The individual components capture market- and instrument-specific stress symptoms, such as increased market volatility, default risk premia, or liquidity risk premia.

The distinctive feature of the CISS is its focus on the *systemic* dimension of financial stress. Systemic stress is interpreted as an *ex post* measure of systemic risk, i.e. a measure of the degree to which systemic risk materialised. It builds on standard definitions of systemic risk characterising it as the risk that financial instability becomes so widespread that it severely disrupts the provision of financial services to the broader economy with significant adverse effects on growth and employment; see e.g. [de Bandt and Hartmann \(2000\)](#) and [Freixas et al. \(2015, p. 13\)](#). The CISS operationalises the idea of systemic stress by aggregating market-specific subindexes of stress based on time-varying correlations between them in the same way portfolio risk (variance) is computed from the risk profiles of individual assets (variances and covariances). In this way the CISS puts more weight on situations in which stress prevails in several market segments at the same time. This is consistent with the idea that stress becomes systemic when it is correlated and widespread. Table [C.1](#) provides a description of all CISS components.

The CISS is computed as follows. First, 15 stress indicators are selected from five major segments of the financial system. The five market segments are i) the financial intermediaries sector, ii) money markets, iii) bond markets, iv) equity markets (only nonfinancial stocks), and v) foreign exchange markets. Taken together, these segments cover the main financial flows from lenders to ultimate borrowers. The financial funds are allocated either directly via securities markets, or indirectly through financial intermediaries.

Second, all indicators are transformed by applying a probability integral transform (PIT) based on their empirical cumulative distribution function. For this purpose, the  $T$  observations of an indicator  $x_t = (x_1, x_2, \dots, x_T)$  are first ranked in ascending order, i.e.  $x_{[1]} \leq x_{[2]} \leq \dots \leq x_{[T]}$ , where  $x_{[1]}$  represents the sample minimum and  $x_{[T]}$  the maximum. The transformed indicators  $z_t$  result from replacing each original observation  $x_t$  with its respective empirical cumulative distribution function value  $F(x_t)$ . That value can be computed as the ranking number  $r$  of observations not exceeding a particular value  $x_t$ , divided by the total number of observations  $T$ .

$$z_t = F(x_t) := \begin{cases} \frac{r}{T} & \text{for } x_{[r]} \leq x_t < x_{[r+1]}, r = 1, 2, \dots, T - 1 \\ 1 & \text{for } x_t \geq x_{[T]}. \end{cases} \quad (\text{C.1})$$

The transformation results in indicators which are unit-free and unconditionally uniformly distributed over the unit interval. The transformed indicators are thus homogenous in terms of scale and distribution. The PIT also robustifies the composite indicator to outliers. This is an important property since the CISS is computed recursively over an expanding data window from January 2002 onwards. For each market segment  $i = 1, 2, \dots, 5$ , we compute a stress subindex  $s_{it}$  from  $j = 1, 2, 3$  transformed components  $z_{ijt}$  as a simple arithmetic average:  $s_{it} = \frac{1}{3} \sum_{j=1}^3 z_{ijt}$ .

Finally, the last aggregation step requires an estimate of time-varying cross-correlations between the  $s_{it}$ . We estimate the variance-covariance matrix  $H_t$  of the 5-dimensional vector of demeaned subindexes  $\tilde{s}_t = (s_t - 0.5)$  as an exponentially-weighted moving average (EWMA), according to which

$$H_t = \lambda H_{t-1} + (1 - \lambda) \tilde{s}_t \tilde{s}_t', \quad (\text{C.2})$$

with a smoothing parameter fixed at  $\lambda = 0.93$ . This is a common choice for daily or weekly data; see Engle (2002). The elements  $\omega_{ijt}$  of correlation matrix  $\Omega_t$  are computed from the elements  $h_{ijt}$  of  $H_t$  as  $\omega_{ijt} = h_{ijt} / \sqrt{h_{iit} h_{jjet}}$ . The CISS is now computed as

$$CISS_t = (w \cdot z_t)' \Omega_t (w \cdot z_t), \quad (\text{C.3})$$

where  $0 < CISS_t \leq 1$  by construction. The vector of market segment weights  $w$  is given in the last column of Table C.1 and is chosen to be approximately in line with euro area national accounts and preliminary data analysis; see [Hollo et al. \(2012\)](#) for details.

Table C.1: Components of the CISS

A listing of variables and transformations used in the computation of the CISS. Volatility is computed as a weekly average of absolute daily log return or interest rate changes. CMAX computed based on end-of-week values. All other series are computed as weekly averages of daily data. Data start in January 1980 or when becoming available. Data sources are Thomson Financial Datastream, ECB, and own calculations. Weekly updates of the CISS are available from the ECB's Statistical Data Warehouse. The SDW key is CISS.D.U2.Z0Z.4F.EC.SS.CI.IDX.

Sector and variables	weight
A. Money markets	0.15
A.1 Volatility of 3-month Euribor.	
A.2 Spread between 3-month Euribor and French Treasury bill rate.	
A.3 Monetary Financial Institutions' recourse to the ECB's marginal lending facility divided by total reserve requirements.	
 B Bond markets	 0.15
B.1 Volatility of German 10-year benchmark government bond prices.	
B.2 7-year yield spread between A-rated nonfinancial corporate and government bonds.	
B.3 10-year interest rate swap spread.	
 C. Equity markets	 0.25
C.1 Volatility of non-financial stock price index.	
C.2 Maximum cumulated loss (CMAX) of non-financial stock price index over a moving 2-year window; $CMAX_t = 1 - x_t / \max[x_i \in (x_{t-j}   j = 0, 1, \dots, 104)]$ .	
C.3 Stock-bond return correlation between total market stock price index and German 10-year government bonds. Computed as difference between moving 4-week and 4-year windows to account for trend changes. Negative differences are set to zero.	
 D. Financial intermediaries	 0.30
D.1 Volatility of financial stock price index.	
D.2 Geometric average of the CDF-transformed CMAX and the book-price ratio associated with a financial stock price index.	
D.3 7-year yield spread between A-rated financial and non-financial corporate bonds.	
 E. Foreign exchange markets	 0.15
E.1 Volatility of euro exchange rate vis--vis US dollar.	
E.2 Volatility of euro exchange rate vis--vis Japanese Yen.	
E.3 Volatility of euro exchange rate vis--vis British pound.	

## **C.2 Financial cycle indicator details**

This subsection sketches the construction of [Schüler et al. \(2019\)](#)'s broad financial cycle indicator for convenience. For details we refer to the original paper.

The indicator is constructed as follows. First, quarterly growth rates of total credit volume, real estate prices, equity prices, and bond prices are obtained. Second, the four series are combined using the CISS methodology as detailed in Section [C.1](#). This approach ensures that the indicator emphasizes times when all four sub-indicators take high values simultaneously. Third, the resulting time series is smoothed by taking a weighted average over a rolling window covering the last six quarters. The weights decline linearly, with the highest weight on the most recent observation. The latter step serves to trade off reliability (fewer erratic movements) against timeliness (ability to react to recent developments in a timely fashion). The indicator is shown to have out-of-sample early warning properties viz-à-viz financially led downturns.

## **C.3 Variable selection: data list and transformations**

Table [C.2](#) reports all macro-financial variables used in our variable selection exercise in Section [4.1](#). We provide a description and the source. Non-stationary time series were detrended using [Hamilton \(2018\)](#)'s regression filter.

**Table C.2: Variables list for the selection exercise**

We report all variables used for our variable selection exercise in Section 4.1. We provide a description and the data source.

Variable	Description	Source
Total employment	Euro area total employment, calendar and seasonally adjusted. Number of persons (Thousands)	Euro area Wide model
Unemployment rate	Euro area unemployment rate, share of civilian workforce, seasonally Adjusted (%)	Euro area Wide model
Gross household savings rate	Euro area gross household saving rate, calendar and seasonally adjusted.	Euro area Wide model
10-year Government bond yield	Euro area nominal Long-Term Interest Rate, Percent Per Annum	Euro area Wide model
3-Month Euribor	Euro area Nominal Short-Term Interest Rate, Last Trade Price, Percent Per Annum	Euro area Wide model
Loans to HHs and Non-profit orgs	Euro area Loans to Households and Non-Profit Organisations Serving Households, Current Prices, Market Value, Euro (Billions)	Euro area Wide model
Loans to Non-Financial corporations	Euro area Loans to Non-Financial Corporations, Current Prices, Market Value, Adjusted for Breaks, Euro (Billions)	CEPREMAP
Capacity utilization rate	Euro area Total Manufacturing Capacity Utilization Rate, Seasonally Adjusted, Monthly Average EA19 (%)	DATASTREAM
House price index	Euro area Residential Property Price Index, Real Value (2015=100)	OECD
House price index - DPI ratio	Euro area Residential Property Price Index-to-Per Capita Net Nominal Disposable Income Ratio (%)	OECD
Standardised House price index-DPI ratio	Euro area Standardised Residential Property Price Index-to-Per Capita Net Nominal Disposable Income Ratio (%)	OECD
House price index, EA17	Euro area Residential Property Price Index, Real Value (2015=100), EA17	OECD
House price index-DPI ratio, EA17	Euro area Residential Property Price Index-to-Per Capita Net Nominal Disposable Income Ratio. EA17 (%)	OECD
Standardised House price index-DPI ratio, EA17	Euro area Standardised Residential Property Price Index-to-Per Capita Net Nominal Disposable Income Ratio. EA17 (%)	OECD
House price index - rent price index ratio, EA17	Euro area Residential Property Price Index-to-Rent Price Index Ratio. EA17 (%)	OECD
Standardised house price index - rent price index ratio, EA17	Euro area Standardised Residential Property Price Index-to-Rent Price Index Ratio. EA17 (%)	OECD
Systemic risk indicator (Median)	Median of the systemic risk indicator. EA19	ECB
Systemic risk indicator (Mean)	Mean of the systemic risk indicator. EA19	ECB
Broad financial cycle indicator	Broad Financial Cycle Indicator	Schueler, Hiebert and Peltonen (2019)
Narrow financial cycle indicator	Narrow Financial Cycle Indicator	Schueler, Hiebert and Peltonen (2019)
10-year US-Euro area interest rate spread	10-Year US Euro Area interest rate differential, Spread, End of Period, Percent per Annum	ECB
EURO STOXX 50 price index	EURO STOXX 50 Price Index, Monthly Average	ECB
Current account balance	EA Current Account Balance as a Share of GDP. EA19 (%)	ECB
News-based economic policy uncertainty index	European Economic Policy Uncertainty Index: News Index (Mean=100)	

## **D Additional results for euro area data**

### **D.1 Robustness to adopting a restricted (linear) specification**

We recompute Figure 5 based on a slope-restricted QVAR model and compare it to the original version in qualitative terms.

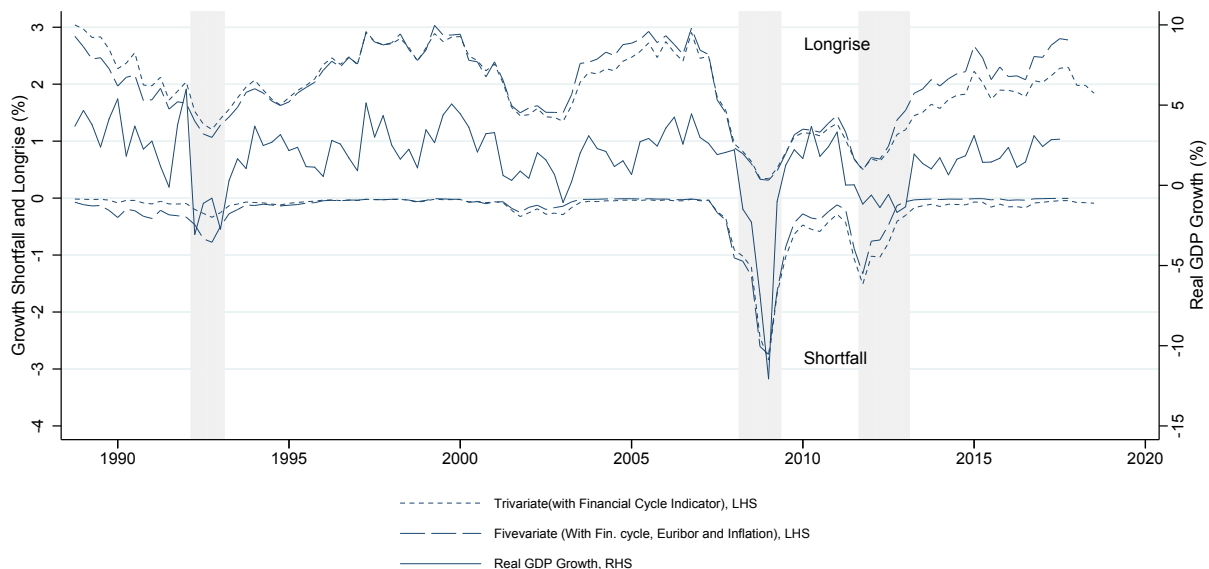
## D.2 Robustness to extending the QVAR information set to five variables

This section considers an alternative five-variable QVAR model specification. The extended model contains quarterly changes in the GDP deflator (inflation) and the three-month EURIBOR interest rate as additional endogenous variables. The monetary policy rate is ordered last, as the central bank sets it in a systematic, forward-looking way (that is, however, not modeled further). The quarterly changes in the GDP deflator are ordered first, and thus does not react contemporaneously to the other four variables.

Figure D.1 plots downside risk (average future growth shortfall) based on the extended five-variable model. Our baseline AGS estimates are provided as a point of comparison; see Figure 5. Both model specifications yield broadly similar predictions in terms of downside risk. We therefore proceed with the above more parsimonious trivariate model for simplicity.

**Figure D.1: Average future growth shortfall estimates for euro area data**

Growth shortfall estimates based on a five-variable QVAR including, in addition, quarterly changes in the log GDP deflator (i.e., inflation) and the three-month EURIBOR interest rate as additional endogenous variables. Our baseline growth shortfall estimates are provided as a point of comparison; see Figure 5. Shaded areas indicate CEPR recessions. The estimation sample is 1988Q3 to 2018Q4.

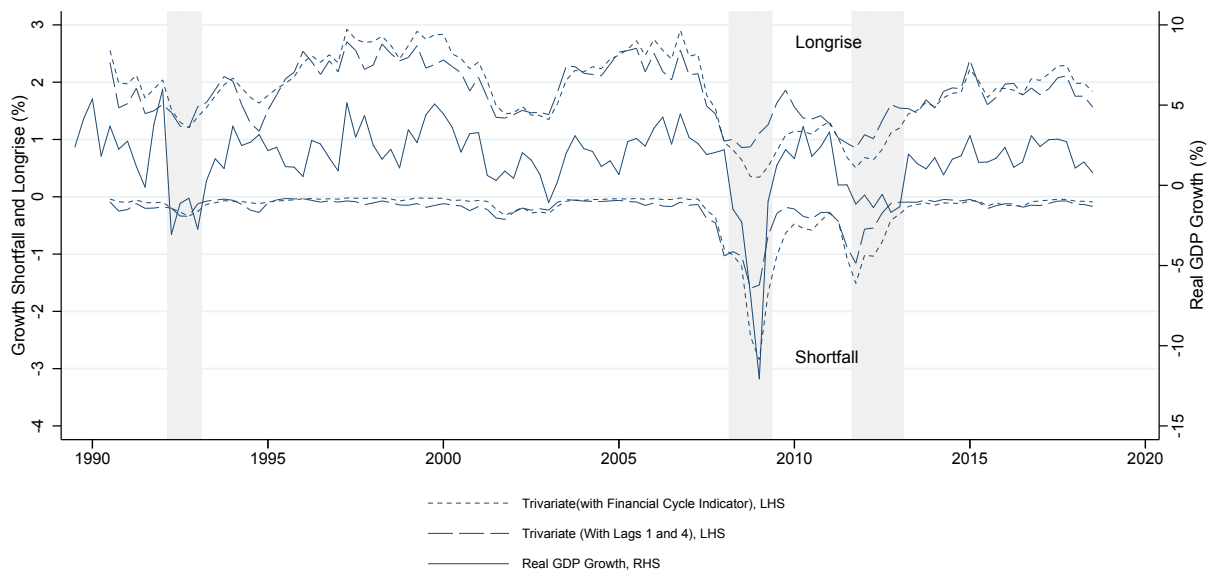


### D.3 Robustness to changes in lag length

This section considers an alternative model specification with an extended lag structure. The alternative model retains the baseline three variables as endogenous variables, but allows for an additional lag at the fourth quarter ( $q = 1, 4$ ). Figure D.2 is analogous to Figure 5. Information criteria prefer the more parsimonious version. Average future growth shortfall responds more quickly, and more severely, to contemporaneous financial stress when based on a single-lag specification.

**Figure D.2: Average future growth shortfall estimates for euro area data**

Growth shortfall estimates based on a three-variable QVAR with an extended lag structure ( $q = 1, 4$ ). Our baseline growth shortfall estimates are provided as a point of comparison; see Figure 5. Shaded areas indicate CEPR recessions. The estimation sample is 1988Q3 to 2018Q4.

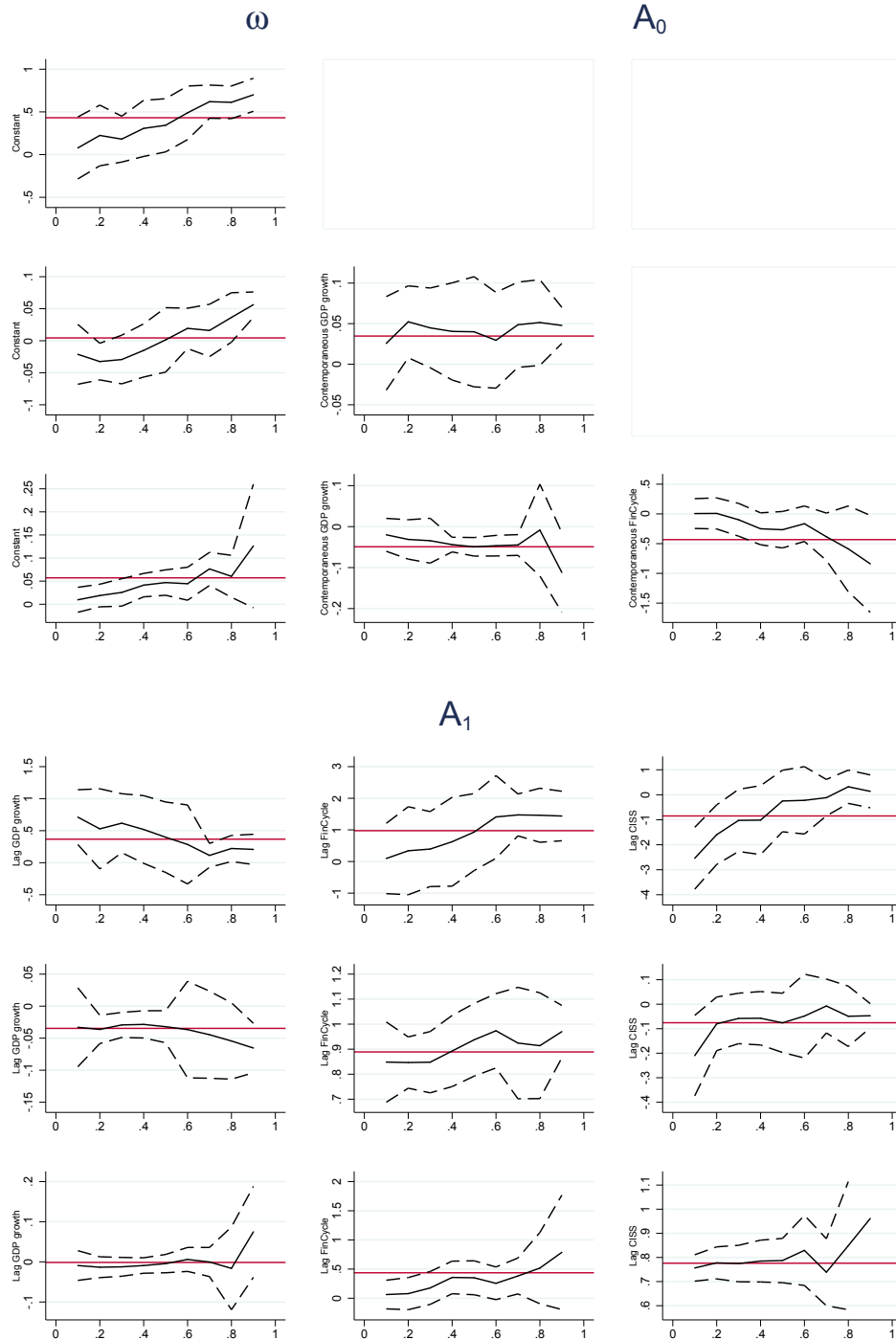


#### **D.4 Parameter estimates from a restricted sample**

Figure 3 reports our baseline QVAR parameter estimates when the estimation sample is restricted to exclude counterfactual pre-1999 euro area data. The point estimates are more noisy but overall similar. The standard error bands are wider, suggesting less precise parameter estimates.

### Figure D.3: Parameter estimates for 1999Q1 – 2018Q4 restricted sample

Parameter estimates from a trivariate QVAR model estimated for  $p = 9$  quantiles from 0.1 to 0.9. Estimation sample is 1999Q1 to 2018Q4. Variables are ordered GDP growth (respective first row), financial cycle (second row), and CISS (third row). Parameter estimates are obtained equation-by-equation while standard error estimates take cross-equation restrictions into account; see Web Appendix B.1. Standard error bands are dashed and at a 95% confidence level. Red horizontal lines indicate least squares estimates.

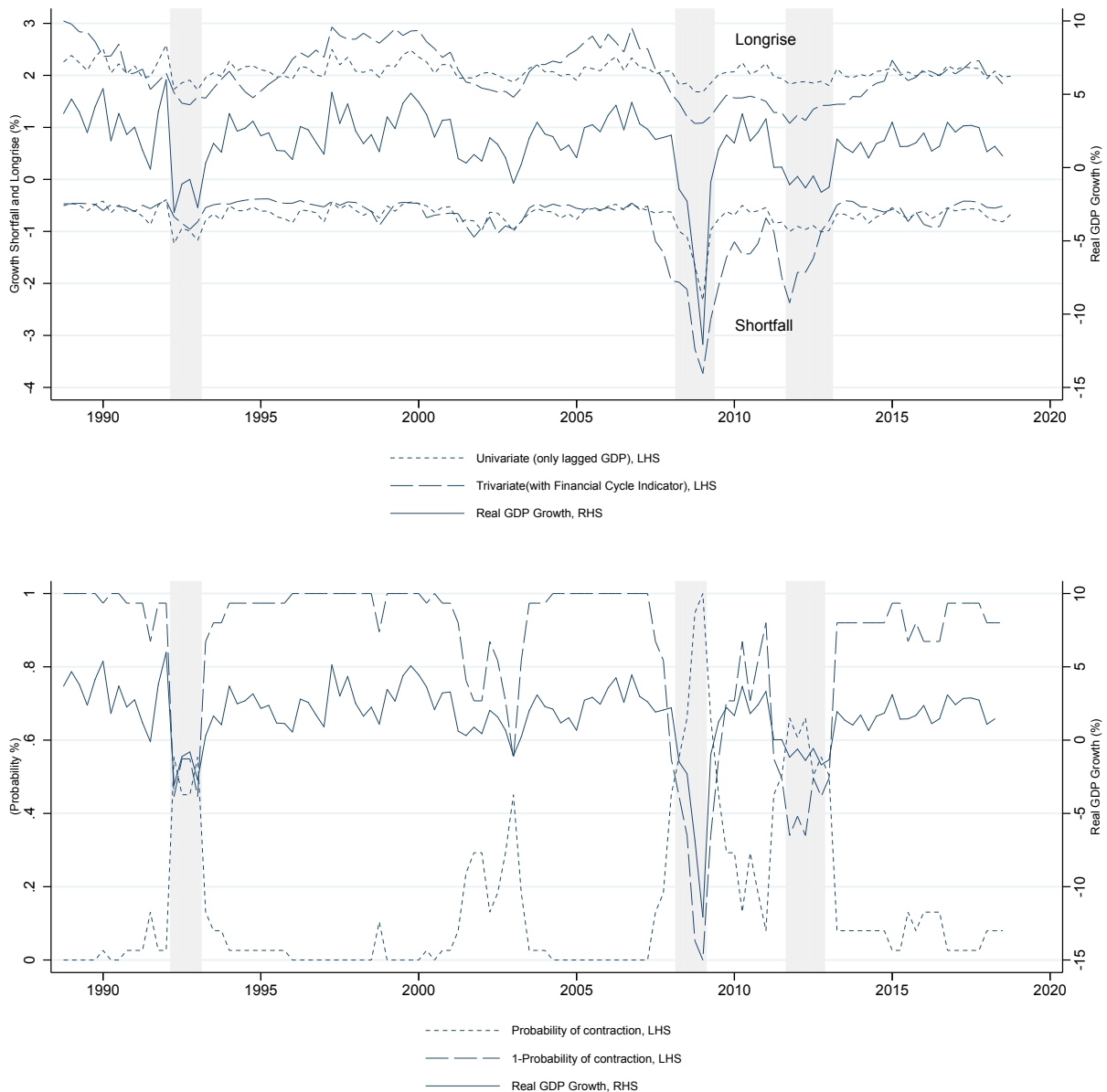


## D.5 Tail conditional expectation and contraction probability

Time- $t$  average future growth shortfall  $AGS_{t,t+1:t+8}^{\tau}$ , and average future growth longrise  $AGL_{t,t+1:t+8}^{\tau}$  consist of two factors: a tail conditional expectation term, and the probability of a contraction; see (2) and (4). The top and bottom panel of Figure D.4 plot the first and second factor over time, respectively. Most of the variability in  $AGS_{t,t+1:t+8}^{\tau}$  comes from the first term, with an additional contribution of the second term in bad times.

### Figure D.4: Euro area AGS and AGL components

Top panel: average future conditional tail expectation; see first factor in (2) and (4). Bottom panel: average future contraction probability; see second factor in (2) and (4). Each estimate is based on  $p = 20$  quantiles ranging from 0.025 to 0.975. The threshold  $\tau$  is set to zero; see Figure 5. We compare these estimates to quarterly annualized real GDP growth (solid line, left scale). Shaded areas indicate euro area recessions as determined by the CEPR business cycle dating committee. The estimation sample is 1988Q3 to 2018Q4.



## E Selected results for U.S. data

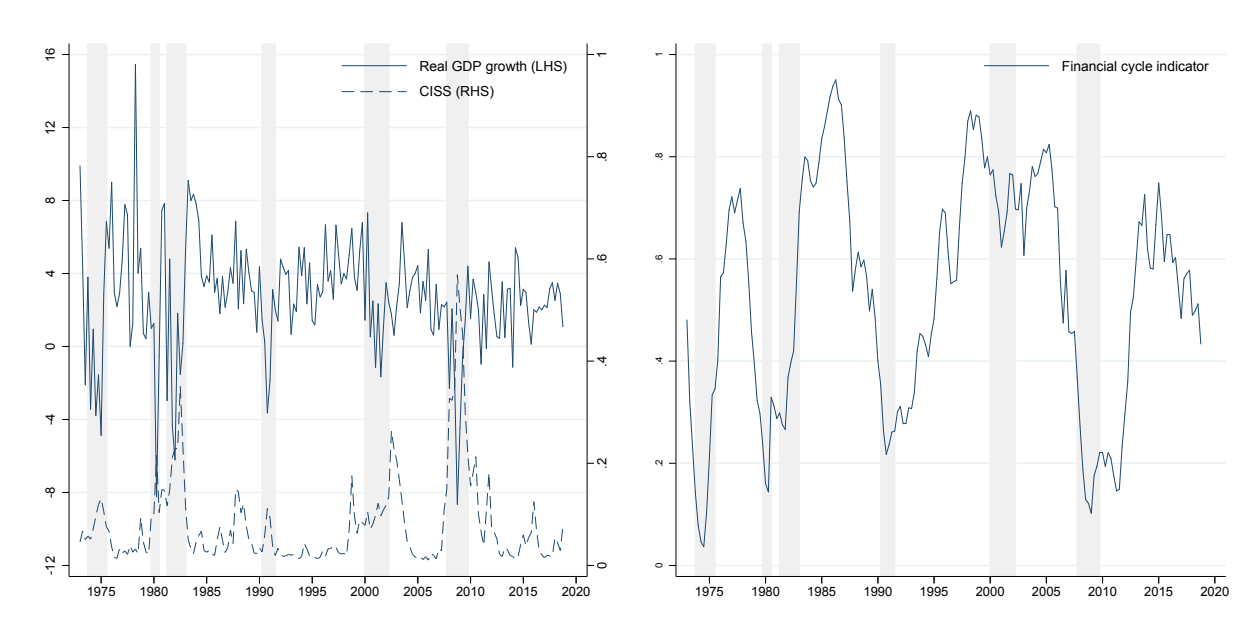
### E.1 U.S. data

The left panel of Figure E.1 reports U.S. quarterly annualized real GDP growth along with the CISS between 1973Q1 and 2018Q4. Shaded areas indicate recession periods according to the NBER business cycle dating committee. High values of the CISS are clearly associated with negative realizations of real GDP growth.

The right panel of Figure E.1 plots Schüler et al. (2019)'s broad financial cycle indicator for the U.S. Their indicator took high values in the years leading up to the U.S. savings and loan crisis during 1982 and 1984, during the dot-com boom years between 1997 and 2000, and during the “conundrum” period between 2003 and 2006 preceding the financial crisis.

**Figure E.1: U.S. real GDP growth rate, CISS, and financial cycle indicator**

The GDP growth rate is annualized. Shaded areas indicate NBER recession periods. CISS and FCY vary between 0 and 1 by construction.



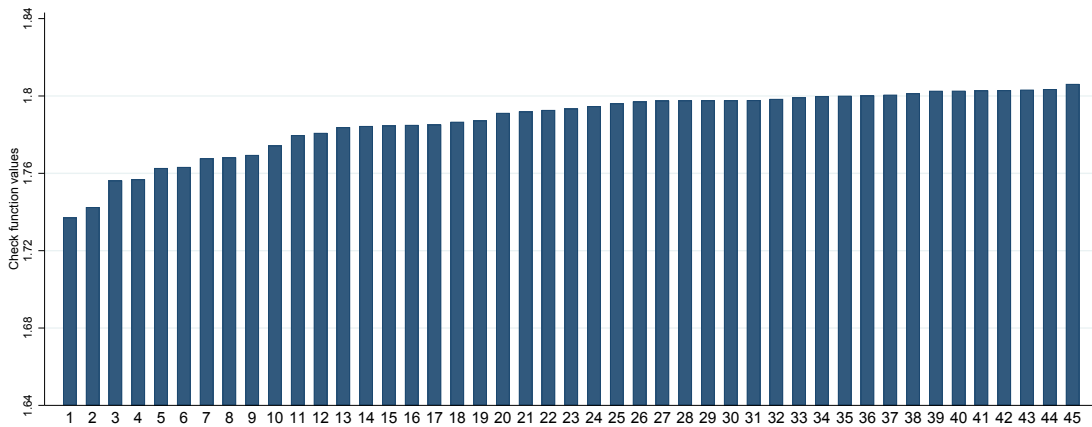
## E.2 Variable selection results

This section reports the results from a variable selection exercise for U.S. data. The setup of the exercise is analogous to the one presented in Section 4.1. We study which variable is most appropriate to be added to a baseline bivariate QVAR containing real GDP growth and U.S. CISS.

Figure E.2 presents our variable selection results. Remarkably, the highly-ranked variables are relatively similar. The broad financial cycle estimate of [Schüler et al. \(2019\)](#) is found to interact closely with U.S. real GDP growth, as well as the U.S. version of the CISS. Short-term and long-term interest rates (implicitly, the term spread) appear to matter as well. The NFCI favored by [Adrian et al. \(2020\)](#) is ranked highly because it is closely related to the U.S.-version of the CISS.

### Figure E.2: Variable selection for U.S. data

Variables are ranked according to their average check function value in a three-variable Q-VAR. Real quarterly GDP growth (ordered first) and the U.S. CISS (ordered last) remain fixed inputs in the three-variable system. The middle variable is looped over. Check function variables are evaluated at quantiles from 0.1 to 0.9 (decile-by-decile) for the GDP growth and CISS equation only. Estimation sample is 1976Q2 to 2018Q4. Non-stationary time series were de-trended using [Hamilton \(2018\)](#)'s regression filter ( $q = 8, h = 2$ ) and are marked with a star.



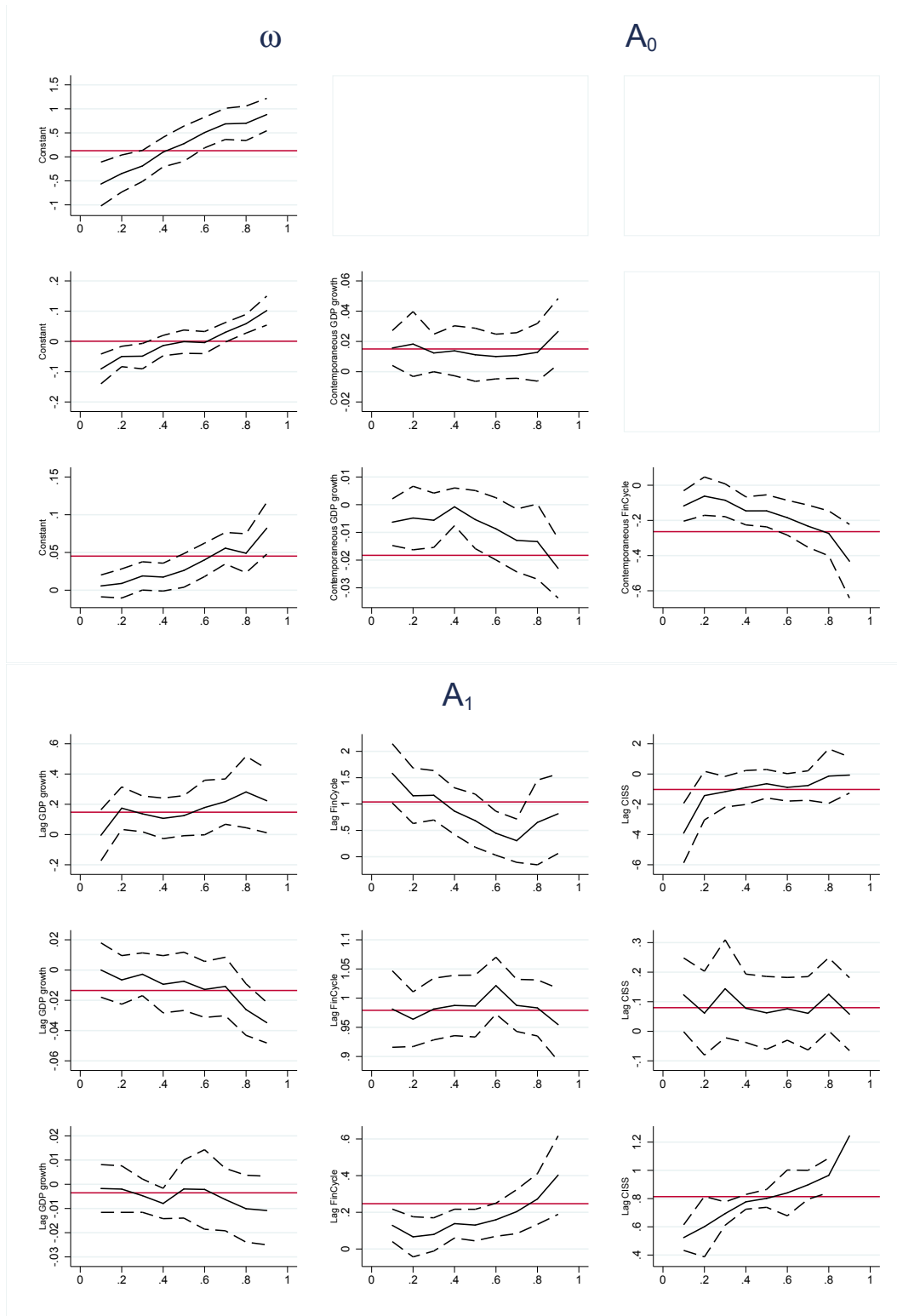
- |  |  |   |
|--|--|---|
| 1 NFCI by Fed Chicago*                           | 2 Financial Cycle Indicator*             | 3 10Y Constant Maturity Rate, Nominal Terms         |
| 4 10Y Constant Maturity Rate, Real Terms         | 5 10Y-Fed Fund Rate Spread*              | 6 Fed Fund Rate                                     |
| 7 Credit to Non-Fin Sector                       | 8 Government Debt                        | 9 Credit to Non-Fin Sector-to-GDP                   |
| 10 Unemployment Rate*                            | 11 New Construction Expenditure          | 12 Home Mortgage Debt                               |
| 13 NFC Debt                                      | 14 S&P500 Price Volatility Index*        | 15 Government Debt/GDP                              |
| 16 Non-Fin Corporations Debt/Equities            | 17 Excess Bond Premiums*                 | 18 Non-Farm Employees                               |
| 19 New Private Construction Expenditure          | 20 Home Mortgage Debt/GDP                | 21 Current Account Balance/GDP                      |
| 22 Consumer Credit                               | 23 Shiller PE Ratio for S&P 500          | 24 Avg Existing Home Price/Income                   |
| 25 HHolds and Non-Profit Org Home Mtg (% Income) | 26 Capacity Utilization Rate*            | 27 Systemic Risk Indicator (d-SRI)*                 |
| 28 HHolds and Non-Profit Org Home Mtg            | 29 NFC Debt/Net Worth                    | 30 Brokers and Dealers' Financial Leverage          |
| 31 NFC Savings                                   | 32 Fin Sector Liabilities/GDP            | 33 HHolds and Non-Profit Org Leverage               |
| 34 HHolds and Non-Profit Org Savings             | 35 HHolds and Non-Profit Org Liabilities | 36 HHolds and Non-Profit Org Liabilities (% Income) |
| 37 Federal Government Fiscal Balance (4Q-MA)*    | 38 Current Account Balance               | 39 NFC Leverage                                     |
| 40 NFC Savings/GDP*                              | 41 Brokers and Dealers' Capital Ratio    | 42 Credit to Non-Fin Sector/GDP Gap*                |
| 43 Avg Existing Home Price                       | 44 Commercial Bank Loan/Deposit          | 45 HHolds and Non-Profit Org Savings/GDP            |

### **E.3 Parameter estimates**

Figure [E.3](#) reports parameter and standard error estimates for our favorite trivariate specification based on U.S. data. The arrangement of panels in Figure [E.3](#) corresponds to the ordering of variables in [\(6\)](#).

### Figure E.3: Parameter estimates for baseline QVAR model

Parameter estimates from a trivariate QVAR model estimated for  $p = 9$  quantiles from 0.1 to 0.9. Parameter estimates are obtained equation by equation while standard error estimates take cross-equation restrictions into account; see Web Appendix A.1. SE banks are at a 95% confidence level. Estimation sample is 1976Q2 to 2018Q4.



## E.4 Wald test and quantile impulse response functions

Table E.1 reports the outcome of three Wald tests of parameter homogeneity across quantiles. We implement the Wald  $\chi^2$  test as explained in Koenker (2005, Ch. 3.3.2); see also Koenker and Basset (1982). The Wald test strongly rejects the pooling (parameter homogeneity) restrictions implied by a linear specification for the GDP growth and CISS equation for U.S. data. The pooling restrictions are not rejected for the financial cycle equation. The test outcomes are intuitive given the parameter and standard error estimates reported in Figure E.3.

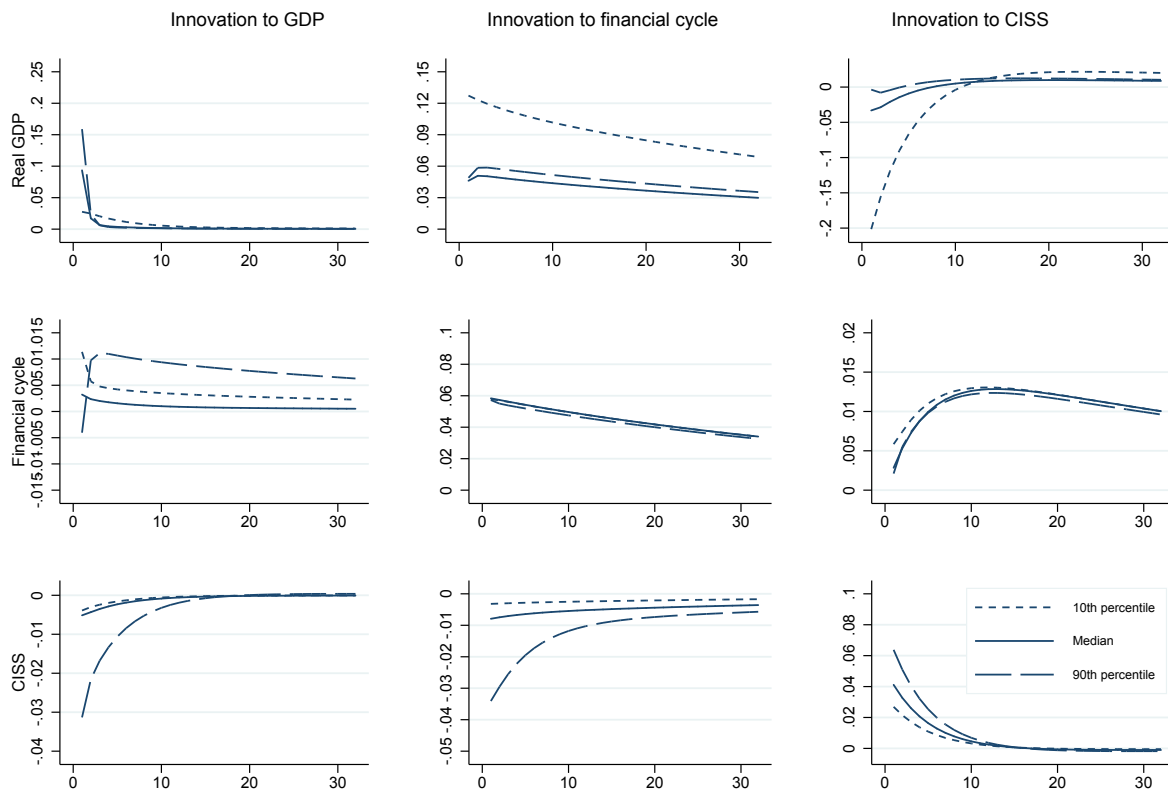
**Table E.1: Wald test for slope homogeneity.**

Wald tests statistics. We consider our baseline trivariate QVAR model, estimated decile-by-decile ranging from 0.1 to 0.9; see Figure E.3. The null hypothesis states that the parameter estimates across the  $p = 9$  quantiles are equal to the median estimates. The test statistic is  $\chi^2$ -distributed. The test statistic's degrees-of-freedom (df) is given by the number of right-hand-side variables per equation (excluding the constant, i.e. 3, 4, and 5, respectively) times the number of imposed restrictions ( $9 - 1 = 8$ ).

	df	test statistic	p-value
real U.S. GDP growth $y_t$	24	66.38	0.00
U.S. financial cycle indicator $c_t$	32	39.25	0.18
U.S. CISS financial stress index $s_t$	40	152.87	0.00

### Figure E.4: Quantile impulse response functions

Impulse response functions implied by the parameter estimates reported in Figure E.3. Variables are ordered as GDP growth (respective first row), U.S. financial cycle (second row), and U.S. CISS (third row). Estimation sample is 1973Q1 to 2018Q4.



## E.5 Growth shortfall estimates

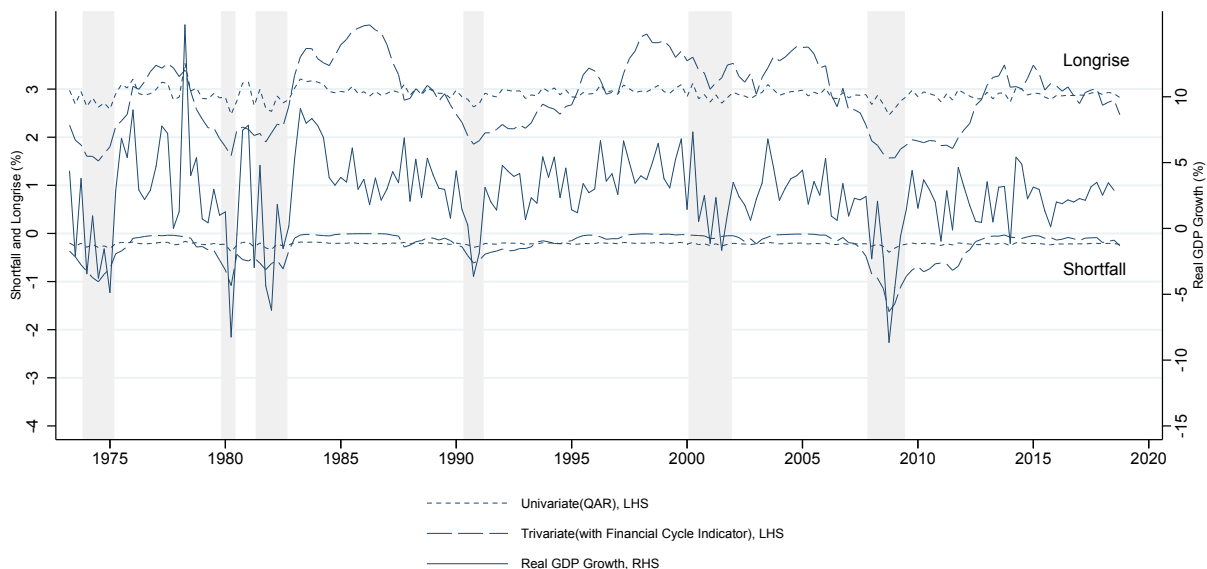
Figure E.5 plots our estimates for average future growth shortfall (AGS) and longrise (AGL) based on U.S. data. Each estimate is based on full-sample estimates, but is otherwise conditional on variables observed up time  $t$ , covering the next two years  $t + 1, \dots, t + 8$ .

The main findings are identical to the ones based on euro area data. There is a pronounced difference between the AGS estimate implied by a univariate QR autoregressive model and the baseline trivariate QVAR. The latter takes financial conditions into account, while the former does not.

Time- $t$  average future growth shortfall ( $AGS_{t,t+1:t+8}^{\tau}$ ) and average future growth longrise ( $AGL_{t,t+1:t+8}^{\tau}$ ), evaluated at  $\tau = 0$  and as reported in Figure E.5, consist of two factors: a tail conditional expectation term, and the probability of a contraction; see (2) and (4). The top and bottom panel of Figure E.6 plot the first and second factor over time, respectively. Most of the variability in  $AGS_{t,t+1:t+8}^{\tau}$

**Figure E.5: Growth shortfall estimates for US data**

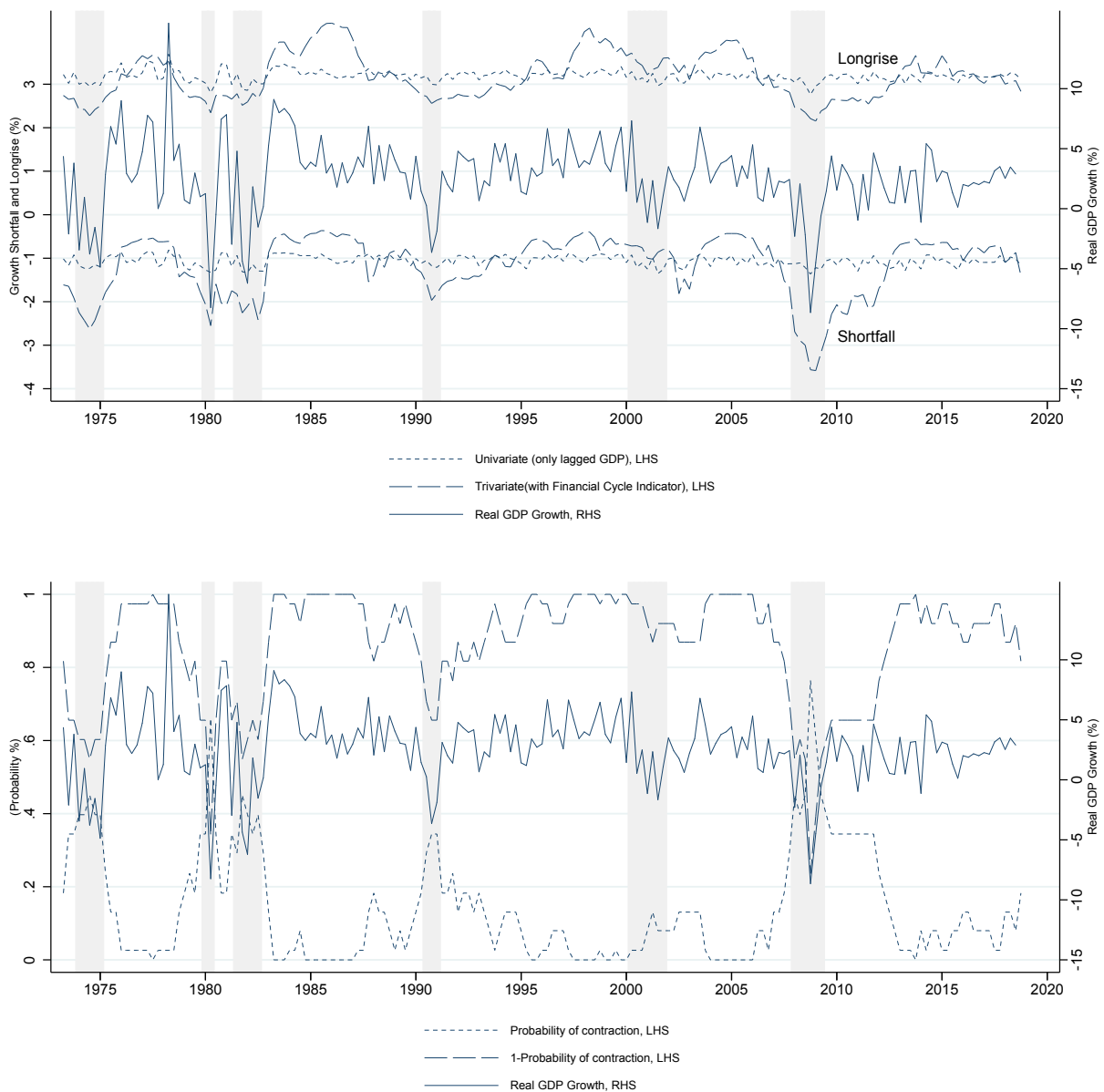
Growth shortfall estimates based on a three-variable Q-VAR. We estimated a different set of parameters for quantiles ranging from 0.1 to 0.9 (decile-by-decile). Shaded areas indicate NBER recessions. The estimation sample is 1973Q1 to 2018Q4.



comes from the first term, with an additional contribution of the second term in bad times.

### Figure E.6: US AGS and AGL components

Top panel: average future conditional tail expectation; see first factor in (2) and (4). Bottom panel: average future contraction probability; see second factor in (2) and (4). Each estimate is based on  $p = 20$  quantiles ranging from 0.025 to 0.975. We compare these estimates to quarterly annualized real GDP growth (solid line, left scale). Shaded areas indicate US recessions as determined by the CEPR business cycle dating committee. The estimation sample is 1973Q1 to 2018Q4.

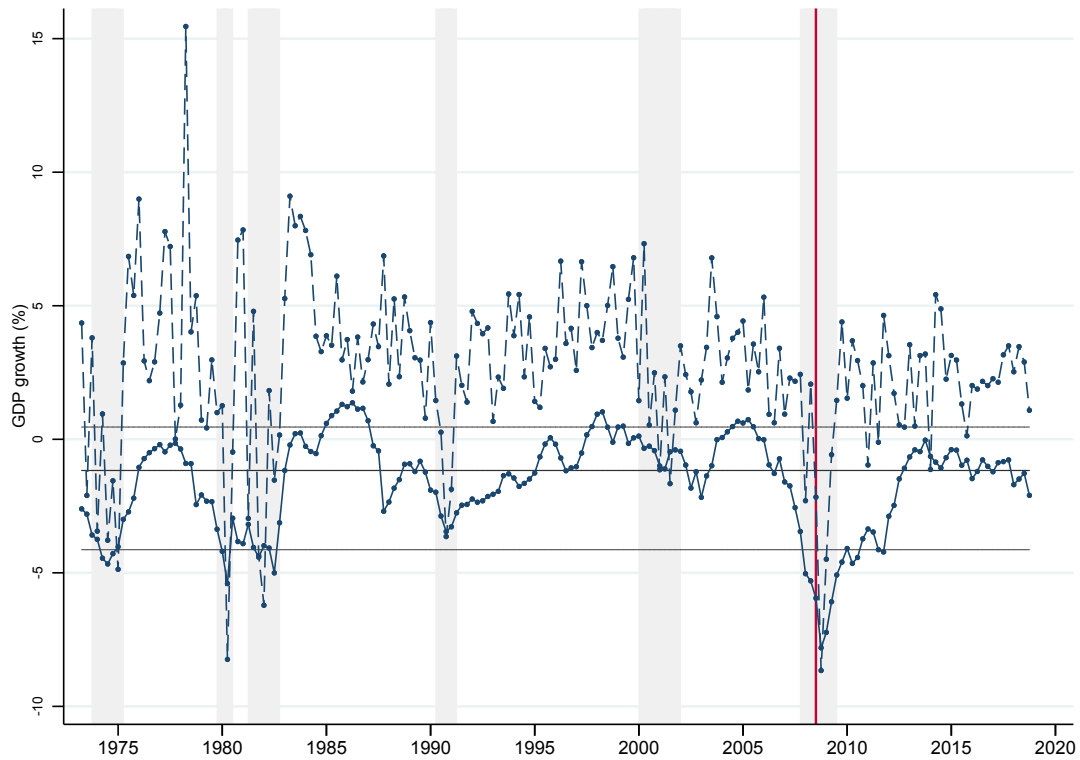


## E.6 Model-based stress testing

Figure E.7 reports the time- $t$  conditional forecast of average future real GDP growth  $\bar{\hat{y}}_{t,t+1:t+8}$  between time  $t$  and  $t + 8$  as implied by our trivariate model. The forecast is conditional on a 0.1 (conditional) quantile realization for GDP growth  $y_{t+h}$ , a 0.1 quantile realization of the financial cycle  $c_{t+h}$ , and a 0.8 quantile realization for CISS  $s_{t+h}$ , consecutively for  $h = 1, \dots, 8$ . The magnitude of these shocks is approximately in line with the eight observed quantile realizations for all variables between 2008Q1 and 2009Q4. The stress test is repeated at each  $t = 1, \dots, T$ , and always based on the same (full sample) parameter estimates. As a result, the figure is informative about the impact of GFC-sized real and financial shocks on real living standards at any time in our sample.

**Figure E.7: Vulnerability to GFC-sized shocks**

Dashed line: U.S. annualized quarterly real GDP growth. Solid line: predicted average annualized quarterly real GDP growth  $\hat{y}_{t,t+1:t+8}$  two years ahead conditional on consecutive 0.1 quantile realizations for GDP growth  $y_t$ , 0.1 quantile realizations of the financial cycle  $c_t$ , and 0.8 quantile realizations for CISS  $s_t$ . Predictions are based on full sample parameter estimates. Estimations sample 1973Q1 – 2018Q4. Horizontal lines refer to 0.1, 0.5, and 0.9 empirical quantiles of  $\hat{y}_{t,t+1:t+8}$ . The vertical line indicates the Lehman Brothers bankruptcy in 2008Q3.



## E.7 The benefits from active policy

The top left, top right, and bottom left panels in Figure E.8 compare real-world U.S. data with counterfactual model-based outcomes for real GDP growth, financial cycle, and financial stress. The final panel presents Kernel estimates of the distribution of real GDP growth in either case. Expected growth is *higher* in the counterfactual scenario. In addition, economic growth is more stable (less volatile around its mean) and less skewed to the downside in the counterfactual scenario.

Table E.2 reports descriptive statistics for the real-world GDP growth sample (left column) and its counterfactual counterpart (right column). Extremely negative and extremely positive realizations for GDP growth disappear from the counterfactual sample. Both mean and median are higher in the counterfactual sample.

Figure E.9 plots the utility difference  $\Delta u_t = u_t(\text{active}) - u_t(\text{passive})$  associated with adopting an active macro-prudential policy.

**Table E.2: Comparison actual vs. counterfactual US growth rates**

Left column: actual quarterly annualized real GDP growth for the US. Right column: counterfactual data assuming that a policy maker could reset the financial cycle to its median conditional value at any time. Estimation sample is 1973Q1 to 2018Q4.

	Real GDP growth	Counterfactual GDP growth
Moments		
Mean	2.649	2.868
Std. Dev.	3.079	2.274
Variance	9.478	5.172
Skewness	-.369	-.041
Kurtosis	5.761	2.719
Percentiles		
1%	-8.242	-2.159
5%	-2.964	-1.169
10%	-1.131	-.012
50%	2.935	2.782
90%	6.463	5.961
95%	7.325	6.695
99%	9.102	7.640
Smallest values		
1st	-8.655	-2.939
2nd	-8.242	-2.159
3rd	-6.214	-2.157
4th	-4.869	-1.947
Largest values		
4th	8.345	7.462
3rd	8.995	7.624
2nd	9.102	7.640
1st	15.457	8.006

### Figure E.8: Leaning against the U.S. financial cycle

Top left panel: actual quarterly annualized real GDP growth for the U.S., and counterfactual data assuming that a policy maker could reset the financial cycle to its conditional median at any time. Top right panel: actual and counterfactual values for the financial cycle. Bottom left panel: actual and counterfactual values for financial stress. Bottom right panel: Kernel estimate over a histogram of actual and counterfactual real GDP growth.

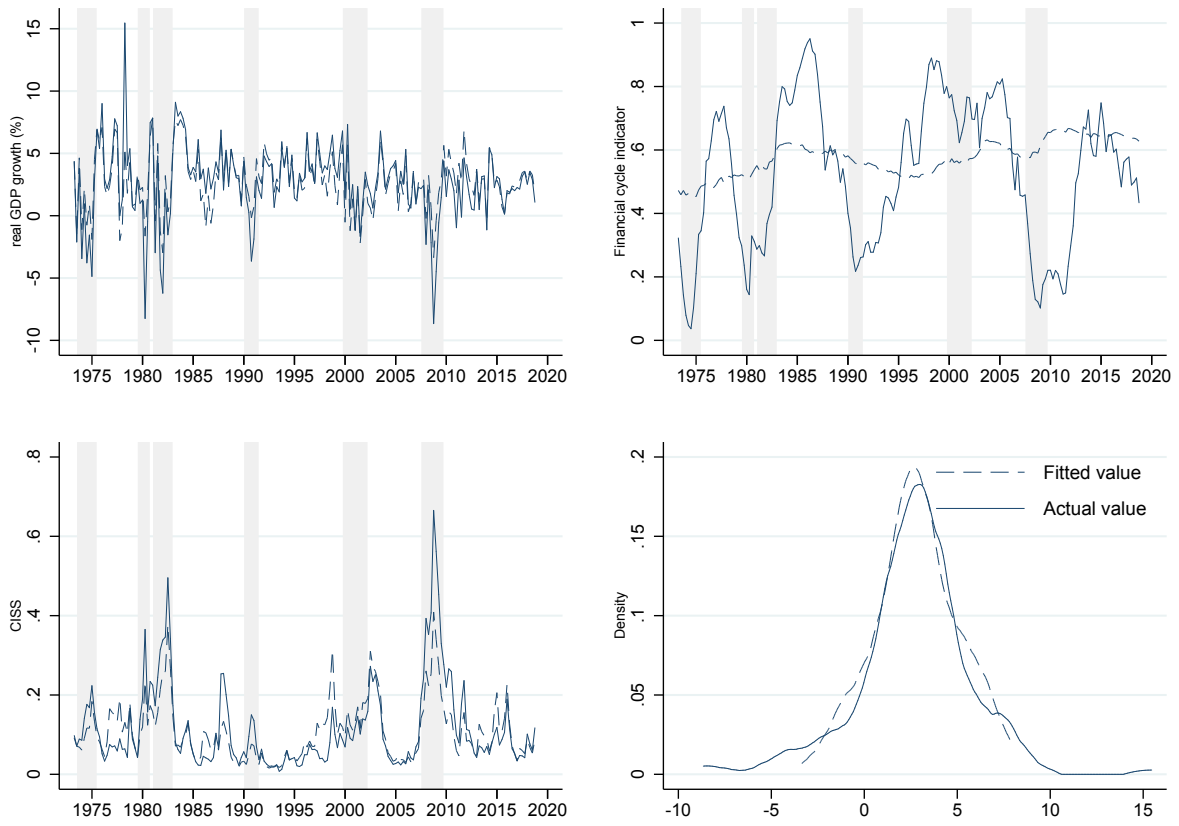
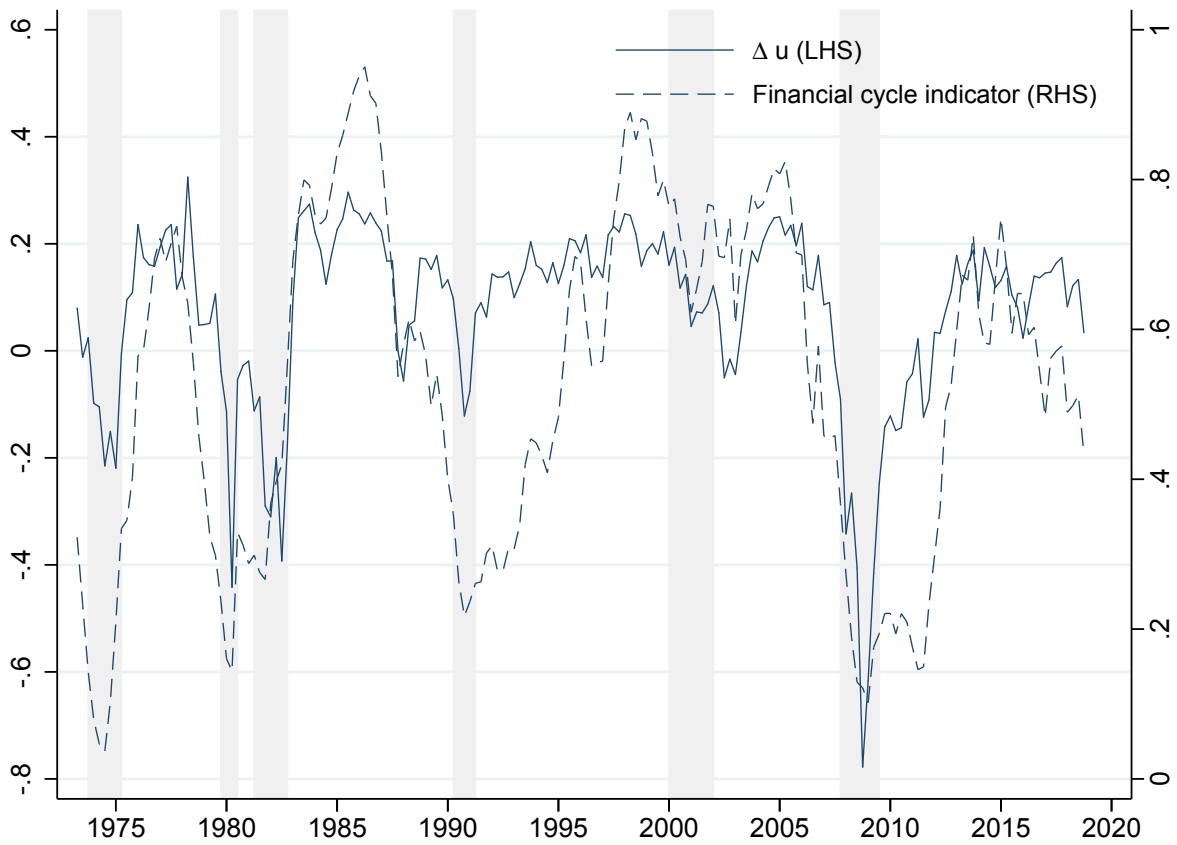


### Figure E.9: The positive benefits from macro-prudential policy

The benefit of adopting a less passive macro-prudential policy stance in utility terms,  $\Delta u_t = u_t(\text{less passive}) - u_t(\text{passive})$ ; see (19). Parameters are chosen as  $\beta = 1$ ,  $\lambda = 1.25$ ,  $\tau = 0$ , and  $H = 12$ . The difference is based on full sample estimates. Estimation sample is 1973Q1 to 2018Q4. Shaded areas indicate U.S. recessions.



## References

- Adrian, T., N. Boyarchenko, and D. Giannone (2020). Multimodality in macro-financial dynamics. *NY Fed staff reports 903*, 1–54.
- de Bandt, O. and P. Hartmann (2000). Systemic risk: a survey. *ECB working paper 35*.
- Engle, R. F. (2002). Dynamic conditional correlation: a simple class of multivariate generalized autoregressive conditional heteroskedasticity models. *Journal of Business and Economic Statistics 20*(3), 339–350.
- Freixas, X., L. Laeven, and J.-L. Peydró (2015). *Systemic risk, crises, and macroprudential regulation*. MIT Press.
- Hamilton, J. D. (2018). Why you should never use the Hodrick-Prescott filter. *Review of Economics and Statistics 100*, 831–843.
- Hollo, D., M. Kremer, and M. L. Duca (2012). CISS – A composite indicator of systemic stress in the financial system. *ECB Working Paper 1426*.
- Illing, M. and Y. Liu (2006). Measuring financial stress in a developed country: an application to Canada. *Journal of Financial Stability 2*(4), 243–265.
- Kliesen, K. L., M. T. Owyang, and E. K. Vermann (2012). Disentangling diverse measures: a survey of financial stress indexes. *Federal Reserve Bank of St. Louis Review 94*(5), 369–398.
- Koenker, R. (2005). *Quantile Regression*. Cambridge: Cambridge University Press.
- Koenker, R. and G. Basset (1982). Robust tests for heteroscedasticity based on regression quantiles. *Econometrica 50*, 43 – 61.
- Schüler, Y., P. Hiebert, and T. A. Peltonen (2019). Financial cycles: Characterisation and real-time measurement. *Journal of International Money and Finance, forthcoming*.
- White, H., T. H. Kim, and S. Manganelli (2015). VAR for VaR: Measuring tail dependence using multivariate regression quantiles. *Journal of Econometrics 187*, 169–188.